

## B. STRUCTURE OF NUCLEI AT THE LIMITS OF STABILITY

The study of the properties of nuclei at the very limits of stability is currently a subject of great interest. Gammasphere was installed at the target position of the FMA late in 1997. A vigorous research program taking advantage of the unique capabilities brought about by the coupling of the two devices has developed since, accounting for a large fraction of the available beam time. In particular, the technique of recoil decay tagging has been used with success to investigate nuclei near or at the proton drip line. Spectroscopy information is now available on states produced at the sub-microbarn level. Other experiments have taken advantage of other auxiliary detectors such as microball and/or the neutron array. This section also presents results of studies where Gammasphere was used to explore nuclei located either along the valley of stability or on the neutron-rich side. Most of these studies used either Coulomb excitation of radioactive, actinide targets or spectroscopy following fission.

### b.1. Spectroscopy of $^{24}\text{Mg}$ Using Gammasphere (C. J. Lister, M. P. Carpenter, D. J. Henderson, A. M. Heinz, R. V. F. Janssens, I. Wiedenhöver, and A. H. Wuosmaa)

In the first year of operation of Gammasphere at ANL, a promising experiment was performed using the Fragment Mass Analyzer as a zero-degree time-of-flight reaction spectrometer. Using two-body reactions the time-of-flight method allowed the selection of individual states which were directly populated from the reaction. The  $^{12}\text{C}(^{16}\text{O}, ^{24}\text{Mg})$  reaction was ideal for this purpose. The technique was found to be particularly sensitive for states which are particle-unbound, but have small radiative branches, perhaps

$10^{-4}$  of their total width. The sensitivity arises as a surviving  $^{24}\text{Mg}$  ion is detected in the final channel. A follow-up experiment was performed in which Gammasphere was used as a full calorimeter, with the data from the 700 BGO elements retained on tape for analysis. This increases the experimental sensitivity by a factor five. The increase should especially enhance the ability to reconstruct high energy gamma-ray information. These data have still to be evaluated.

### b.2. First Identification of a $10^+$ State in $^{24}\text{Mg}$ (I. Wiedenhöver, A. H. Wuosmaa, H. Amro, J. Caggiano, M. P. Carpenter, A. Heinz, R. V. F. Janssens, F. G. Kondev, T. Lauritsen, C. J. Lister, S. Siem, A. Sonzogni, P. Bhattacharyya,\* M. Devlin,† D. G. Sarantites,† and L. G. Sobotka†)

The level structure of  $^{24}\text{Mg}$  provides a crucial testing ground for theoretical approaches as different as the spherical shell model or  $\alpha$ -cluster descriptions. High-spin states with  $I \approx 8$  are especially sensitive to the assumptions underlying the different models. To identify candidate states with  $I \approx 8$  we performed an experiment at ATLAS using a high granularity Si strip array with 160 channels inside the target chamber of Gammasphere. The states of interest in  $^{24}\text{Mg}$  were populated in the  $^{12}\text{C}(^{16}\text{O}, ^{24}\text{Mg})$  reaction. The  $\alpha$ -particles emitted from the compound nucleus, the subsequent  $\alpha$ -decay to states of  $^{20}\text{Ne}$  and the characteristic  $\gamma$ -rays emitted from the  $^{20}\text{Ne}$  nucleus were observed in coincidence.

The technique for spin determination is based on the observation of the fivefold directional correlations

between the beam axis, the two  $\alpha$  particles and two photons, which are emitted in the decay path leading from the compound state in  $^{28}\text{Si}$  ( $m = 0$ ) to the ground state of  $^{20}\text{Ne}$  (see Fig. I-12). The main concept of the method is illustrated by Fig. I-12. All steps of one individual decay path, i.e. two  $\alpha$  and two  $\gamma$  rays must be observed in the event in order to produce a characteristic angular correlation, which permits a spin determination. If one gamma ray of the decay path remains unobserved, the  $\alpha$  particles lose their characteristic correlations and spin determination becomes impossible. The necessity of detecting events with high efficiency lead to the design of a compact experimental setup of 5 DSSD detectors in the target chamber of Gammasphere.

The other difficulty in this project lay in the data analysis: In order to determine the correlation patterns of this five dimensional problem, a new technique was developed that relies on the expansion into coefficients of an orthogonal basis and allows the concentration of the relevant information into only few spectra. Employing this technique, we were able to assign spins to nine levels and confirm previous assignments unambiguously. The most notable result is the

identification of a  $10^+$  state at 19.1 MeV (see Fig. I-14). The first unambiguous identification of this level in  $^{24}\text{Mg}$  resolves a long-standing problem of nuclear physics. The energy of the  $10^+$  state lies on the continuation of the ground state rotational band, indicating that the rotational sequence continues far beyond the  $-$ binding threshold. This  $10^+$  state is with  $\hbar$  2.9 MeV one of the fastest rotating nuclear systems ever observed.

\*Purdue University, †Washington University

<sup>1</sup>R. K. Sheline, I. Ragnarsson, S. Aberg, and A. Watt, Jrnl. Phys. G **16**, 1201 (1988).

<sup>2</sup>S. Marsh and W. D. M. Rae, Phys.Lett. **B180**, 185 (1986).

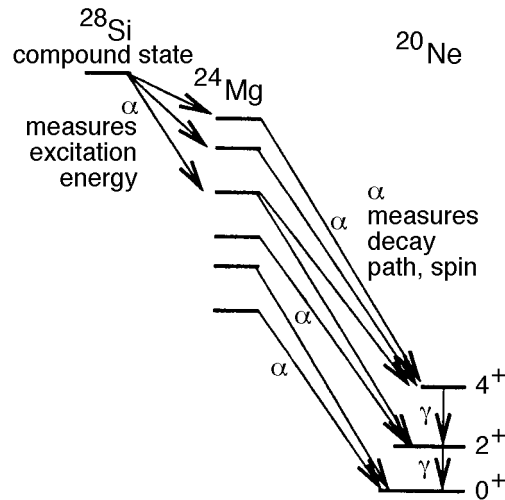


Fig. I-12 Schematic decay path from the  $^{28}\text{Si}$  ( $m = 0$ ) state to the ground state of  $^{20}\text{Ne}$ .

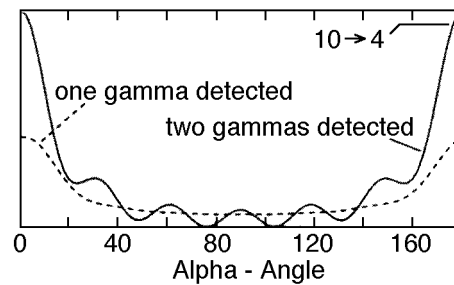


Fig. I-13 Angular distributions calculated for the emission of an  $\alpha$ -particle from a  $10^+$  state of  $^{24}\text{Mg}$  populating the  $4^+$  state of  $^{20}\text{Ne}$ . Solid line: in coincidence with two  $\gamma$ -rays, detected at  $(\theta, \phi) = (45^\circ, 0)$  and  $(45^\circ, 180^\circ)$ . Dashed line: in coincidence with only one  $\gamma$ -ray at  $(\theta, \phi) = (45^\circ, 0)$  (dashed line), not observing the  $4^+ \rightarrow 2^+$  transition.

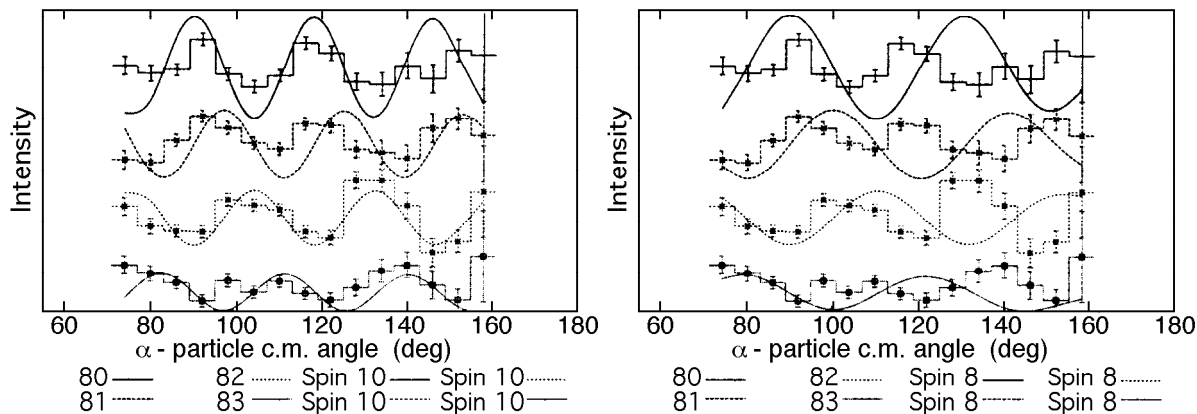


Fig. I-14 Experimental correlated angular distributions of  $\alpha$ -particles  $^{24}\text{Mg}$ , 19.1 MeV  $^{20}\text{Ne}$  ( $4^+$ ), compared to the theoretical curves for spin  $10^+$  (left) and  $8^+$  (right). Plotted are the correlations with the  $(k,q) = (8,0), (8,1), (8,2), (8,3)$  components of the patterns detected with Gammasphere.

**b.3. Deformed Excitations in  $^{71}\text{As}$  and  $^{72}\text{Br}$**  (M. P. Carpenter, C. J. Lister, C. N. Davids, R. V. F. Janssens, D. Seweryniak, T. L. Khoo, T. Lauritsen, D. Nisius, P. Reiter, J. Uusitalo, I. Wiedenhoever, N. Fotiades,\* J. A. Cizewski,\* A. O. Macchiavelli,† and R. W. MacLeod‡)

The nuclei in the  $A = 70$  mass region exhibit a complicated interplay between single-particle and collective degrees of freedom, reflecting the influence of competing shell gaps in the single-particle levels. As a result, gamma sequences built on configurations corresponding to different shapes are observed in the same nucleus, e.g.  $^{72}\text{Se}$ <sup>1</sup>. In order to understand better the single-particle excitations responsible for the deformed structures, we have recently studied with Gammasphere the level structure of  $^{71}\text{As}$  and  $^{72}\text{Br}$ .

High-spin states in both  $^{71}\text{As}$  and  $^{72}\text{Br}$  were investigated using the  $^{16}\text{O} + ^{58}\text{Ni}$  reaction at a beam energy of 59.5 MeV. The  $^{16}\text{O}$  beam was supplied by the ATLAS accelerator at Argonne National Laboratory. Gamma rays at the target position were detected by the Gammasphere array which was coupled to the Fragment Mass Analyzer (FMA) in order to separate evaporation residues from other reaction products. Mass 71 and 72 were the strongest evaporation residue channels observed in this reaction. In addition to  $^{71}\text{As}$  ( $3p$ ) and  $^{72}\text{Br}$  ( $pn$ ),  $^{68}\text{Ge}$  ( $2p$ ),  $^{71}\text{Se}$  ( $2pn$ ),  $^{72}\text{Se}$  ( $2p$ ) have also been identified in this data set.

The previous reported level structure<sup>2</sup> for  $^{71}\text{As}$  has been confirmed and extended in this experiment. In addition, a new sequence of negative-parity levels have been observed at moderate excitation. This sequence consists of two rotational bands connected to each other by dipole transitions which compete favorably with the quadrupole cross-over transitions. Based on the extracted  $B(M1)/B(E2)$ , the band has been given a  $7/2^- [303] (f_{7/2})$  assignment with  $\lambda_2 \sim 0.37$ . This is the first observation of a deformed proton  $f_{7/2}$  configuration in the  $A = 70$  mass region.

\*Rutgers University, †Lawrence Berkeley National Laboratory, ‡Thomas Jefferson National Accelerator Facility

<sup>1</sup>J. H. Hamilton *et al.*, Phys. Rev. Lett. **32**, 239 (1974).

<sup>2</sup>R. S. Zigelboim *et al.*, Phys. Rev. C **50**, 716 (1994).

<sup>3</sup>S. Ulbig *et al.*, Z. Phys. **A329**, 51 (1988).

<sup>4</sup>R. Bengtsson *et al.*, Nucl. Phys. **A415**, 189 (1984).

<sup>5</sup>N. Fotiades *et al.*, Phys. Rev. C **59**, 2919 (1999).

<sup>6</sup>N. Fotiades *et al.*, Phys. Rev. C **60**, 057302 (1999).

For  $^{72}\text{Br}$ , the level scheme deduced in the present study has been extended with respect to previous work<sup>3</sup>. Two of the gamma-sequences observed have been associated with the  $g_{9/2}$   $g_{9/2}$  deformed configuration. The observed signature splitting between the two bands is larger than that observed for similar decoupled bands in the heavier odd-odd Br

isotopes due to the lower-  $= 3/2$ ,  $g_{9/2}$  orbitals involved. In addition, the low-frequency signature inversion observed in the heavier Br isotopes is absent in  $^{72}\text{Br}$  in accordance with theoretical predictions<sup>4</sup>.

Two papers reporting the results from this experiment have been published this past year in Phys. Rev. C<sup>5,6</sup>.

**b.4. Spectroscopy of N = Z  $^{68}\text{Se}$ ,  $^{72}\text{Kr}$ ,  $^{76}\text{Sr}$ ,  $^{80}\text{Zr}$ ,  $^{84}\text{Mo}$  and  $^{88}\text{Ru}$**  (C. J. Lister, M. P. Carpenter, A. M. Heinz, D. J. Henderson, R. V. F. Janssens, J. Schwartz, D. Seweryniak, I. L. Wiedenhöver, J. Cizewski,\* N. Fotiades,\* A. Bernstein,† Becker,† Bauer,† S. Vincent,‡ A. Aprahamian,‡ P. Hausladen,§ D. Balamuth,§ and S. M. Fischer¶)

The nuclei with N = Z above  $^{56}\text{Ni}$  continue to attract attention, because of their importance in understanding explosive nucleosynthesis, and as they are fertile testing ground for nuclear models and for testing fundamental symmetries of nuclear forces. However, the nuclides of greatest interest lie far from stability, sometimes only one nucleon from the proton dripline. The systems are weakly bound and difficult to produce. Only recently has experimental technique advanced sufficiently to allow detailed spectroscopy in the nuclei of greatest interest. A series of experiments have been conducted using Gammasphere to study properties of these nuclei.

A)  $^{68}\text{Se}$  This nucleus was predicted to provide an interesting example of shape coexistence. For many years it has been expected to be one of the few nuclei in nature with substantial ( $\sim -0.3$ ) oblate deformation in its groundstate. An FMA-Gammasphere experiment aimed at low-spin shape coexistence was performed, using the “Daresbury” method of tagging recoils by their stopping properties in an ion chamber. The reaction used,  $^{12}\text{C}(^{58}\text{Ni}, 2n)^{68}\text{Se}$  at the Coulomb barrier is ideal for populating low-spin non-yrast states. Despite the low production cross section of about 200  $\mu\text{b}$ , two bands were found as is shown in Fig. I-15. The bands appear to both be collective, but have very different characteristics, the ground state band appearing to be characteristic of an oblate band while the excited band behaves similarly to the many prolate bands known in the region. The oblate groundstate appears about 600 keV more bound than the prolate shape. However, the prolate configuration has larger moments of inertia, so becomes yrast at spin J = 8. The oblate-prolate barrier is lowest in the triaxial plane at  $\beta = 0.3$ , and is predicted to be a few hundred keV high. The rather weak oblate-prolate mixing found in experiment indicates the barrier is higher than anticipated. These results have been published as a Physical Review Letter. A follow-up experiment by the

Berkeley group using the microball has extended the yrast sequence to higher spin, through a two-alpha evaporation channel. It is clear the FMA gated, 2n evaporation studies and the microball-gated 2 measurements are very complimentary, the former favoring low-cross section, low-multiplicity, low-spin non-yrast structure and the latter high-spin phenomena.

B)  $^{72}\text{Kr}$  At low spin,  $^{72}\text{Kr}$  exhibits signs of coexistence similar to  $^{68}\text{Se}$ , although the prolate shape dominates the yrast landscape and the oblate band could not be identified as it has become non-yrast even by spin J = 2. However, at high spin in the prolate sequence, a new challenge has been pursued. It has been suggested that new neutron-proton collective pairing modes, characteristic only of N = Z nuclei would require greater rotational Coriolis force to destroy, so alignments would be delayed to higher frequency. Two issues arise: what would one expect the “normal” frequency to be, and experimentally how large is the delay? We have performed a microball-Gammasphere experiment and through the  $^{40}\text{Ca}(^{40}\text{Ca}, 2n)^{72}\text{Kr}$  reaction have developed the decay scheme well past the backbending region, to spin J = 28 or higher. We have found the alignment is indeed delayed relative to other krypton isotopes and have identified several new bands. These data are in the final stages of analysis.

C)  $^{76}\text{Sr}$  By N = Z = 38 the oblate shapes are gone and prolate shapes dominate. This should be an ideal place to find further evidence of “delayed alignment” and also quantify the stiffness of this nucleus which is the most deformed in the region with  $\beta = 0.4$ . An experiment has just been completed. Using a new triggering mode, Gammasphere was operated in free-running “singles” mode, interrupted only when a recoil-gamma coincidence was detected in “external” electronic logic. This arrangement substantially

reduced dead time and thus enhanced the size of the data set. On-line sorting indicated it should be possible to extend the yrast line from spin  $J = 4$  to above  $J = 16$ , well past the expected alignment frequency.

D)  $^{80}\text{Zr}$  Another good rotor studied for “delayed alignment”. This was the test experiment for the novel triggering described above. Despite some technical hitches, an excellent data set was collected and the yrast sequence advanced from  $J = 4$  to  $J = 12$ . Clear evidence for delayed alignment was found, as the moment of inertia rises smoothly to the highest identified state, well above the frequency at which alignment is found in the other deformed zirconium nuclei.

E)  $^{84}\text{Mo}$  Formed as a by-product in the  $^{88}\text{Ru}$  study described below, evidence for this nucleus was found at an intensity level sufficient to suggest the structure may

be investigated to higher spin than the  $J = 4$  which is presently known. Analysis is in progress.

F)  $^{88}\text{Ru}$  This nucleus has been sought in many structure studies. To date, no excited states are known. Using the  $^{32}\text{S}(^{58}\text{Ni}, 2n)^{88}\text{Ru}$  reaction and the “Daresbury” method, an attempt was made to elucidate its structure. One challenge was to produce a sulfide target of sufficient robustness to withstand bombardment with about 10 pA of 200 MeV  $^{58}\text{Ni}$ . This has been a stumbling block in previous studies. In this experiment a  $\text{MoS}_2$  target was prepared and mounted on a rotating target wheel. This arrangement was very satisfactory, and after some initial “conditioning” with a small loss of sulfur, the target stabilized for extended running. A substantial data set was collected and data are being analyzed, though ion-chamber gain drifts and dead time issues compromised this data set, which was one of the first in this series of studies.

\*Rutgers University, †Lawrence Livermore National Laboratory, ‡University of Notre Dame, §Pennsylvania University, ¶DePaul University

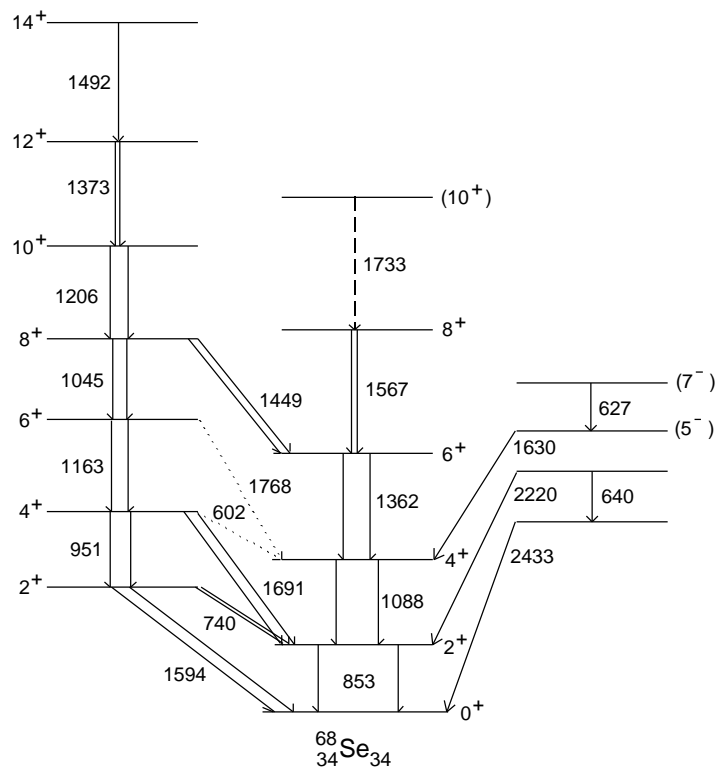


Fig. I-15. The two bands observed in  $^{68}\text{Se}$ . The groundstate band has all the characteristics of an oblate shape, while the excited band is consistent with prolate deformation.

**b.5. Yrast and Near-Yrast Excitations up to High Spin in  $^{100}\text{Cd}$**  (M. P. Carpenter, R. V. F. Janssens, D. Seweryniak, I. Wiedenhöver, R. M. Clark,\* J. N. Wilson,† D. Appelbe,‡ C. J. Chiara,§ M. Cromaz,\* M. A. Deleplanque,\* M. Devlin,† R. M. Diamond,\* P. Fallon,\* D. B. Fossan,§ D. J. Jenkins,¶|| N. Kesall,¶|| T. Koike,§ D. R. LaFosse,§ G. L. Lane,\* I. Y. Lee,\* A. O. Macchiavelli,\* K. Starosta,§ F. S. Stephens,\* C. E. Svensson,\* K. Vetter,\* R. Wadsworth,¶|| J. C. Waddington,‡ D. Ward,\* and B. Alex Brown||)

In recent years, there has been an increasing experimental effort devoted to the study of nuclei near the doubly-magic,  $N = Z$  nucleus,  $^{100}\text{Sn}$ . Gamma-ray spectroscopic studies are edging ever closer to this goal, but the very low (microbarn) cross sections and high backgrounds from other reaction products make it difficult to identify gamma transitions with nuclides produced with these low cross sections.

Recently, we have studied high-spin states in  $^{100}\text{Cd}$  ( $Z = 48, N = 52$ ) a close lying isobar to  $^{100}\text{Sn}$  in order to learn more about the location of single-particle states near  $N = Z = 50$ . In this study, states in  $^{100}\text{Cd}$  were populated in the  $^{46}\text{Ti}(^{58}\text{Ni}, 2p2n)$  reaction with a beam of energy of 215 MeV. Gamma rays emitted at the target were measured with Gammasphere. In order to identify gamma transitions in  $^{100}\text{Cd}$ , the evaporated particles from this reaction were measured using Microball and a 20 element array of NE213 liquid scintillator detectors. The former was used to detect light charged particles while the later was used to detect neutrons. In addition, an Au catcher foil was placed immediately behind the target with the aim of stopping all recoils in order to allow for a tag on delayed transitions coming from isomeric states.

Before this study, excited states in  $^{100}\text{Cd}$  were known up to the 60 ns  $8^+$  isomer<sup>1</sup>. In this study, a prompt  $\gamma$ -ray spectrum consisting of transitions lying above the  $8^+$  isomer was produced by gating on delayed transitions lying below the isomer in coincidence with

the detection of two protons and at least one neutron. To build the level scheme, a  $E - E$  matrix was formed by incrementing events which were in coincidence with any of the four prompt delayed transitions lying below the  $8^+$  isomer. No other gates on evaporated particles were required.

From the analysis of the data, the level scheme of  $^{100}\text{Cd}$  has been extended up to  $20 \hbar$  in angular momentum and 10 MeV in excitation energy. Spin and multipolarity assignments were made based on angular correlation ratios. In an attempt to understand the single-particle nature of the states, shell model calculations were performed and compared with the data. The spectrum of the yrast states up to  $I = 14 \hbar$  is generally well reproduced by the shell-model calculations. Above this spin and excitation energy, high-energy  $\gamma$ -ray transitions are observed. These transitions can be viewed as a "fingerprint" of either core excitations or excitations involving  $h_{11/2}$  neutrons. It is clear that a full quantitative description of the decay scheme requires extended shell-model calculations. Indeed, the recent advances in  $\gamma$ -ray spectroscopy of nuclei near  $^{100}\text{Sn}$  are clearly outstripping the theoretical descriptions and it is our hope that experimental efforts such as presented here will encourage renewed theoretical effort.

A paper reporting the results of this work was published recently in Physical Review C<sup>2</sup>.

\*Lawrence Berkeley National Laboratory, †Washington University, ‡McMaster University, Hamilton, Ontario, §SUNY at Stonybrook, ¶University of York, United Kingdom, ||Michigan State University

<sup>1</sup>Gorska *et al.*, Z. Phys. **A350**, 181 (1994).

<sup>2</sup>R. M. Clark *et al.*, Phys. Rev. C **61**, 044311 (2000).

**b.6. Spectroscopy of  $^{103}\text{Sn}$  and the Development of a Technique to Observe  $^{101}\text{Sn}$** 

(C. J. Lister, M. P. Carpenter, D. Seweryniak, C. Baskill,\* S. Freeman,\* J. Durell,\* B. J. Varley,\* M. Leddy,\* D. Balamuth,† P. Hausladen,† S. Fischer,§ and D. Sarantites‡)

The approach to the doubly-magic nucleus  $^{100}\text{Sn}$  has proven very difficult using fusion evaporation reactions. In “inbeam” spectroscopy  $^{104}\text{Sn}$  is the closest isotope studied, although a high-spin isomer has been found and studied in  $^{102}\text{Sn}$ , yielding the effective charge for neutrons beyond the doubly magic shell closure.

An attempt was made to populate  $^{103}\text{Sn}$  using the  $^{50}\text{Cr}(^{60}\text{Ni}, 3n)$  reaction and using microball, neutron detectors, the FMA and an ion-chamber to over define the reaction products, while gamma rays were detected in Gammasphere. The aim of the experiment was two-fold: evaluation of channel selection techniques in order to plan a future study of  $^{101}\text{Sn}$  using the same reaction but with a  $^{58}\text{Ni}$  beam, and secondly to identify states in  $^{103}\text{Sn}$ , particularly the 3-neutron multiplets to evaluate residual interactions and state mixing.

The data are still undergoing evaluation. The 16-detector Penn-Manchester array of scintillators had an efficiency of about 14% for one neutron, about that achieved using the more recently commissioned UW-LBNL-Penn 30 detector arrangement. However, the neutron-gamma separation was very good. The microball was very clean in identifying alpha particles

downstream, but upstream alphas in this inverse reaction were very difficult to identify efficiently, so the overall detection efficiency was lower than estimated. Buildup of light contaminants on the target was also an impediment to clean channel selection. The efficiency of the FMA was also less than originally estimated, due to its operation at 90 cm, forced by the size of Gammasphere. Very few events had correlated mass  $A = 103$  ions detected at the FMA focal plane and identified alphas in microball due to the alpha-residue angular correlation. Finally, after target and window losses, the ion-chamber resolution was less clean than expected and electronic gain drifts were found which needed correction. Thus, in almost all respects the channel selection techniques were poorer than originally expected. However, many aspects can be worked on and technically improved for the future.

Despite these shortcomings, a very large data set was collected, and a spectrum for  $^{103}\text{Sn}$  may emerge. However, at present the information from this experiment seems most valuable for designing an optimum experiment for the future. Many aspects of the project can be improved and tested without Gammasphere. A Manchester student is pursuing this project for his Ph.D. thesis project.

\*University of Manchester, United Kingdom, †University of Pennsylvania, ‡Washington University, §DePaul University

**b.7. In-Beam  $\alpha$ -Ray Spectroscopy of the Proton Emitter  $^{109}\text{I}$**  (M. P. Carpenter, C. N. Davids, R. V. F. Janssens, C. J. Lister, D. Seweryniak, J. Uusitalo, C. H.-Yu,\* A. Galindo-Uribarri,\* S. D. Paul,\*† and B. D. McDonald‡)

The recoil decay tagging (RDT) technique has proven to be a powerful tool in the study of proton-rich nuclei. With the placement of Gammasphere in front of the FMA, this technique has been successfully used to probe excited states in nuclei which lie at the edges of stability. In the past two years a number of RDT measurements have been performed with the Gammasphere + FMA setup. These studies have attempted to characterize the nuclear structure built on top of the proton emitting states. One such experiment was performed on  $^{109}\text{I}$ , a nuclide which had been studied previously at the Daresbury tandem accelerator

using the EUROGAM I array and the Daresbury Recoil Mass Spectrometer<sup>1</sup>.

In the experiment at Gammasphere, excited states in  $^{109}\text{I}$  were populated using the  $^{54}\text{Fe}(^{58}\text{Ni}, p2n)$  reaction at a beam energy of 220 MeV. Gamma rays in  $^{109}\text{I}$  were identified using the RDT technique. The analysis of the  $\alpha$ -data yielded the yrast sequence in  $^{109}\text{I}$  which has been interpreted as an excitation built on the  $h_{11/2}$  proton orbital. Interestingly, the sequence of gamma-rays assigned to this band in  $^{109}\text{I}$  is different than that reported in Ref. 1. Since the Gammasphere assignments are based on a significantly larger number

of gamma-proton correlated events, we believe that the sequence reported in Ref. 1 is incorrect.

Previous systematic analyses of proton emitters have shown that most known proton emitters have spectroscopic factors close to unity.  $^{109}\text{I}$  stands out as one of the few which have very small spectroscopic factors. The proton emitting ground state of  $^{109}\text{I}$  has been assigned to the  $d_{5/2}$  configuration, however, its spectroscopic factor is very small ( $S = 0.055$ ), and this fact has been cited as evidence that the ground state has

substantial prolate deformation. Unfortunately, the current experiment was unable to identify states associated with the ground state configuration, and thus, no information on the deformation of the ground-state could be extracted. The trend of the  $h_{11/2}$  sequence indicates a decrease in deformation with decreasing  $N$  which is supported by theoretical predictions.

A paper reporting the results of this work was published this past year in Physical Review C.<sup>2</sup>

\*Oak Ridge National Laboratory, †Oak Ridge Institute for Science and Education, ‡Georgia Institute of Technology  
<sup>1</sup>E. S. Paul, P. J. Woods, *et al.*, Phys. Rev. C **51**, 78 (1995).

<sup>2</sup>C. H.-Yu *et al.*, Phys. Rev. C **59**, R1834 (1999).

### b.8. Lifetimes of High-Spin States in Proton Rich A = 130 Nuclei (F. G. Kondev, M. P. Carpenter, A. Heinz, R. V. F. Janssens, D. J. Hartley,\* L. L. Riedinger,\* A. Galindo-Uribarri,† R. W. Laird,‡ W. Reviol,§ M. A. Riley,‡ and O. Zeidan\*)

The mass 130 region is a rich field for shape coexistence phenomena where bands with axial, triaxial, and oblate deformations are present in the vicinity of the yrast line. In addition, highly deformed bands (with  $\beta = 0.3-0.4$ ) are observed in these nuclei which result from the occupation of shape-driving  $i_{13/2}$  and/or  $g_{9/2}$  orbitals as well as from the proximity of neutron shell gaps at higher deformations at  $N = 72, 74$ . A previous experiment was performed with the Gammasphere spectrometer in conjunction with the Washington University Microball charged-particle detection array using the  $^{40}\text{Ca} + ^{94}\text{Mo}$  reaction. Several possible highly deformed structures were identified in

In order to confirm that the new structures have large deformation, a lifetime measurement was recently performed at the ATLAS facility where once again the power of Gammasphere was combined with the selectivity of the Microball. The same reaction was performed, but a target consisting of  $\sim 1 \text{ mg/cm}^2$  of  $^{94}\text{Mo}$  on  $\sim 14 \text{ mg/cm}^2$  of Au was used instead of a self-supporting  $^{94}\text{Mo}$  foil as in the previous experiment. Lifetimes of the states will be extracted by applying a lineshape analysis (Doppler shift attenuation method (DSAM), which will allow us to determine the quadrupole moments (and thus the deformations) of some of these bands. By populating so many highly deformed bands under the same experimental conditions, we are able to compare the deformations of the bands without concern for systematic differences that occur when comparing quadrupole moments deduced in different measurements. The analysis is in progress.

$^{130,131}_{60}\text{Nd}$ ,  $^{127-131}_{59}\text{Pr}$ , and  $^{128,130}_{58}\text{Ce}$  from this experiment.

\*University of Tennessee, †Oak Ridge National Laboratory, ‡Florida State University, §University of Tennessee and Washington University



**b.10. Properties of N = 84 Even-Even Nuclei Populated in the Spontaneous Fission of  $^{248}\text{Cm}$**  (I. Ahmad, A. Korgul,\* W. Urban,\* T. Rzaca-Urban,\* M. Rejmund,\* J. L. Durell,† M. J. Leddy,† M. A. Jones,† W. R. Phillips,† A. G. Smith,† B. J. Varley,† N. Schulz,‡ M. Bentaleb,‡ E. Lubkiewicz,‡ and L. R. Morss§)

Systematic studies of the N = 84 isotones were made in order to test the limits of the region around  $^{132}\text{Sn}$  where the shell-model description still applies. The  $^{134}\text{Sn}$  nucleus, identified in our earlier study, was reinvestigated. The 2509 keV level in  $^{134}\text{Sn}$  obtained in the present work was interpreted as the  $(f_{7/2} h_{9/2})$  configuration. Its excitation energy fits very well the shell-model description, providing further confirmation of the  $h_{9/2}$  single-particle assignment of the 1561-keV level in  $^{133}\text{Sn}$ . On the other hand,  $^{138}\text{Xe}$ , which also has two valence neutrons, displays an excitation pattern characteristic of vibrational, collective motion. This nucleus cannot be described by the shell

model. Between these two limits is  $^{136}\text{Te}$ , having two valence protons and two valence neutrons. The maximum aligned configurations  $[(g_{7/2})^2 0^+ (f_{7/2})^2 6^+]$ ,  $[(g_{7/2})^2 0^+ (f_{7/2} h_{9/2}) 8^+]$  and  $[(g_{7/2})^2 6^+ (f_{7/2} h_{9/2}) 8^+]$  which in  $^{136}\text{Te}$  correspond to the  $6^+$ ,  $8^+$  and  $14^+$  levels are well described by the shell-model code OXBASH. On the other hand the  $[(g_{9/2})^2 6^+ (f_{7/2})^2 6^+]$  configuration is observed at an excitation energy higher than predicted and does not produce the expected isomerism in  $^{136}\text{Te}$ . We explained this difference as the result of collective motion admixtures in  $^{136}\text{Te}$ , only four valence nucleons away from the  $^{132}\text{Sn}$  core. The results of this study were published.<sup>1</sup>

\*University of Warsaw, Poland, †University of Manchester, United Kingdom, ‡IREs, Strasbourg, France, §Chemistry Division, ANL

<sup>1</sup>A. Korgul *et al.*, Euro. Phys. J. **A7**, 167 (2000).

**b.11. Medium Spin Structure of Single Valence-Proton Nucleus  $^{133}\text{Sb}$**  (I. Ahmad, W. Urban,\* W. Kurcewicz,\* A. Korgul,\* P. J. Daly,† P. Bhattacharyya,† C. T. Zhang,† J. L. Durell,‡ M. J. Leddy,‡ M. A. Jones,‡ W. R. Phillips,‡ A. G. Smith,‡ B. J. Varley,‡ M. Bentaleb,§ E. Lubkiewicz,§ N. Schulz,§ L. R. Morss,¶ and J. Blomqvist||)

Excited states in  $^{133}\text{Sb}$  populated in the spontaneous fission of  $^{248}\text{Cm}$  were studied with the EURO GAM2 array. The  $^{133}\text{Sb}$  nucleus, having one valence proton, provides direct information on the single-particle excitations. Its structure can be described as the excitations of the single valence proton coupled to the  $^{132}\text{Sn}$  core. We have identified excited levels in  $^{133}\text{Sb}$  corresponding to the  $(h_{11/2}^{-1} f_{7/2})$  core excitations coupled to the  $g_{7/2}$  proton level. The  $13/2^+$ ,  $15/2^+$  and  $17/2^+$  yrast members of the  $[(g_{7/2} (h_{11/2}^{-1} f_{7/2})]$  configurations were observed. Our calculations give

the energy of the  $19/2^+$  member higher than that of the  $21/2^+$  level, which in turn is predicted to lie only  $\sim 30$  keV above the  $17/2^+$  level. This is the cause for the  $16 \mu\text{s}$  isomerism, reported previously. Another important finding in  $^{133}\text{Sb}$  was the identification of the 4297 keV level, corresponding to the  $3^-$ , octupole vibration of the core. Work is in progress to determine the rate of the E3 transition associated with this excitation. The results of this investigation have been submitted to Phys. Rev. C.

\*Warsaw University, Poland, †Purdue University, ‡University of Manchester, United Kingdom, §IREs, Strasbourg, France, ¶Chemistry Division, ANL, ||Royal Institute of Technology, Stockholm, Sweden

**b.12. First Observation of Excited States in  $^{137}\text{Te}$  and the Extent of Octupole Instability in the Lanthanides** (I. Ahmad, W. Urban,\* A. Korgul,\* T. Rzaca-Urban,\* N. Schulz,† M. Bentaleb,† E. Lubkiewicz,† J. L. Durell,‡ M. J. Leddy,‡ M. A. Jones,‡ W. R. Phillips,‡ A. G. Smith,‡ B. J. Varley,‡ and L. R. Morss§)

Studies of neutron-rich lanthanides have revealed a region of octupole instability around  $N = 88$ . To understand the dependence of octupole correlations on neutron numbers we have studied the structures of heavy Te isotopes. Excited states in  $^{137}\text{Te}$  were investigated in the spontaneous fission of  $^{248}\text{Cm}$  by measuring coincidence spectra with the gamma ray array EUROGAM2. To find transitions in  $^{137}\text{Te}$ , spectra were obtained by placing gates on rays in the complementary Ru fragments. Several new rays were observed. To assign the new transitions to  $^{137}\text{Te}$ , mass correlation technique was used. By gating on transitions in a given Te isotope, the ray intensities of

the Ru isotopes were obtained. The weighted mass of the Ru isotopes was plotted against the mass of each Te isotope. The excellent correlation confirms the assignment of transitions to  $^{137}\text{Te}$ .

The level scheme of  $^{137}\text{Te}$  as deduced from the present work is displayed in Fig. I-17. The structure of  $^{137}\text{Te}$  is similar to those of heavier  $N = 85$  isotones and can be interpreted as due to three valence nucleons in the  $(f_{7/2}^3)_j$  or  $[h_{9/2}(f_{7/2}^2)]_j$  configurations. The data indicate a decrease in octupole correlations as one is approaching  $Z = 50$  shell. The results of this study were published.<sup>1</sup>

\*Warsaw University, Poland, †IReS, Strasbourg, France, ‡University of Manchester, United Kingdom, §Chemistry Division, ANL

<sup>1</sup>W. Urban *et al.*, Phys. Rev. C **61**, 041301(R) (2000).

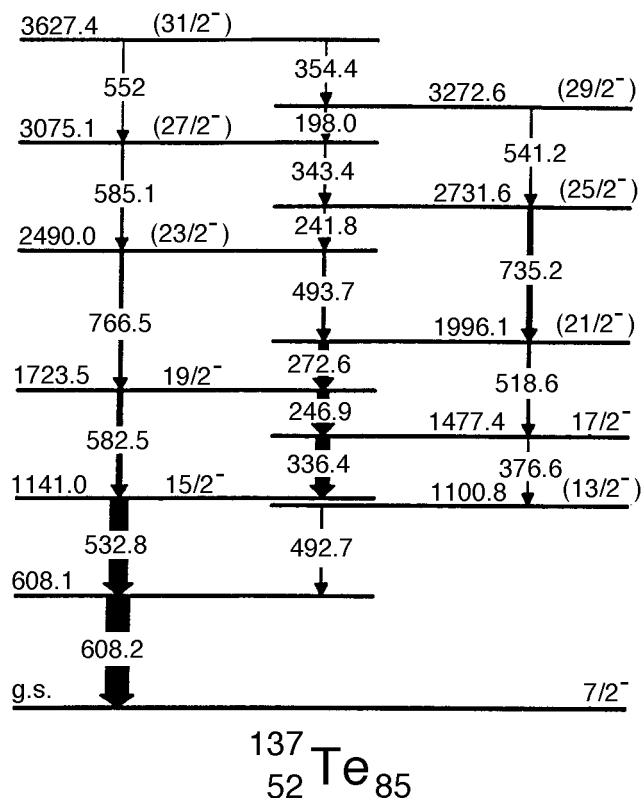


Fig. I-17. The level scheme of  $^{137}\text{Te}$  deduced from the results of the present study.

**b.13. First Observation of Excited States in the Neutron-Rich Nucleus  $^{138}\text{Te}$**  (I. Ahmad, F. Hoellinger,\* B. P. J. Gall,\* N. Schulz,\* W. Urban,† M. Bentaleb,\* J. L. Durell,‡ M. A. Jones,‡ M. Leddy,‡ E. Lubkiewicz,§ L. R. Morss,¶ W. R. Phillips,‡ A. G. Smith,‡ and B. J. Varley‡)

Levels in  $^{138}\text{Te}$  have been observed for the first time. Gamma rays produced in the spontaneous fission of  $^{248}\text{Cm}$  were measured with the EUROAM2 array of Ge detectors. Several new gamma rays were observed in coincidence with the gamma rays of complementary light Ru isotopes. The mass assignment of the new gamma rays was made on the basis of the mass correlation technique. By gating on the transitions in Te isotopes, intensities of gamma rays in the Ru isotopes were measured. The

weighted mass of the Ru isotopes was plotted against the mass of each Te isotope. The excellent correlation, shown in Fig. I-18, confirms the assignment of transitions to  $^{138}\text{Te}$ . The level scheme obtained from the present work is displayed in Fig. I-19. The level scheme indicates a soft prolate minimum consistent with theoretical predictions. The results were published<sup>1</sup>.

\*IREs and Universite Louis Pasteur, Strasbourg, France, †Warsaw University, Poland, ‡University of Manchester, United Kingdom, ¶Chemistry Division, ANL, §Jagiellonian University, Cracow, Poland

<sup>1</sup>F. Hoellinger *et al.*, Eur. Phys. J. A **6**, 365 (1999).

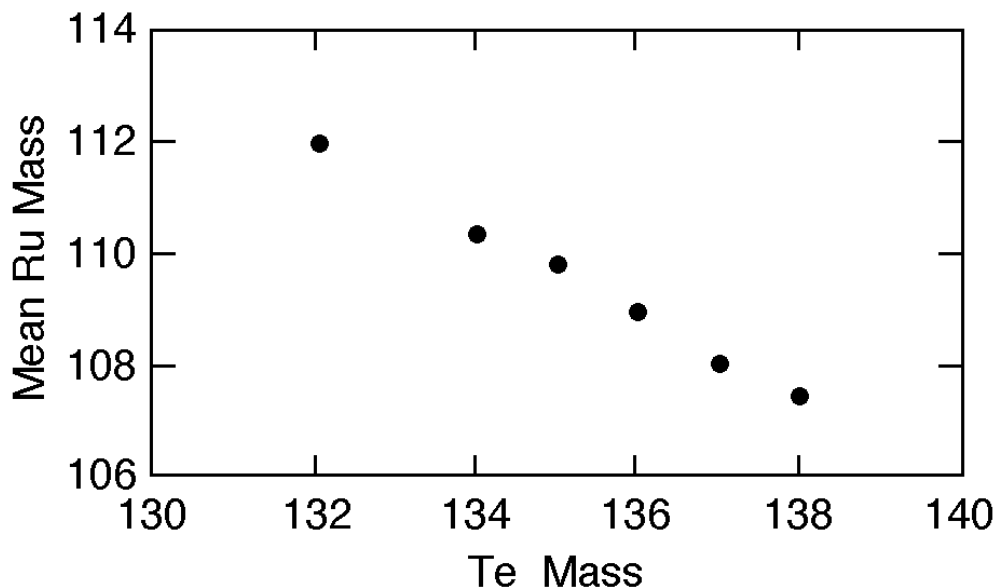


Fig. I-18. Plot of mean mass of Ru isotopes against the mass of the Te isotope. The smooth trend in the data points is the basis for the assignment of new gamma lines to  $^{138}\text{Te}$ .

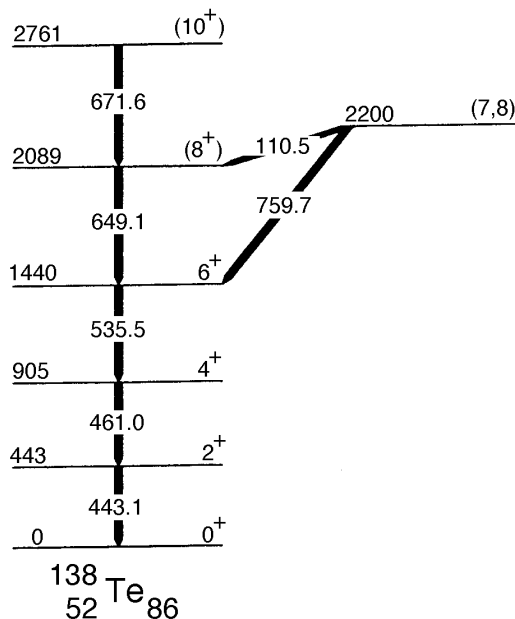


Fig. I-19. Level scheme of  $^{138}\text{Te}$  obtained in the present work.

#### b.14. Measurements of g-Factors of Excited States of Fission Fragments Implanted into Fe

I. Ahmad, M. P. Carpenter, J. P. Greene, R. V. F. Janssens, F. Kondev, D. Seweryniak, A. G. Smith,\* O. J. Onakanmi,\* D. Patel,\* G. S. Simpson,\* J. F. Smith,\* R. M. Wall,\* J. P. Gall,† B. Roux,† and O. Dorveaux†)

An experiment was performed with Gammasphere to measure g-factors of excited states in neutron-rich fission fragments using the time-integral perturbed angular correlation functions between pairs of secondary-fragment rays. The experiment involved the use of a  $^{252}\text{Cf}$  source of total activity  $100\ \mu\text{Ci}$  sandwiched between two layers of Fe metal. Prior to the deposition of the californium, the Fe metal foils (each  $10\ \text{mg cm}^{-2}$  thick) were annealed in an oven at  $650^\circ\text{C}$  for ten minutes. The magnetization of these foils as a function of temperature and applied field was measured using a magnetometer. The results of this measurement showed that the magnetic moment of the iron reached saturation at room temperature in an applied field of 0.1 T. The Cf was then electroplated onto the surface of one of the iron foils and a layer of indium metal ( $200\ \mu\text{g cm}^{-2}$  thick) was evaporated over the second iron foil. A pair of small permanent magnets applying a field of around 0.2 T were placed either side of the source in the direction normally reserved for the beam to Gammasphere. The direction

of the applied field could be reversed by rotating the magnet assembly through an angle of  $180^\circ$ . The experiment ran for two weeks during which time  $9 \times 10^9$  events of fold three (or greater) were collected. A preliminary check on the precessions of angular correlations in the fragments  $^{100}\text{Zr}$ ,  $^{104}\text{Mo}$  and  $^{144}\text{Ba}$  has revealed impurity hyperfine fields of -26(5), -24(3) and -4.5(7) T, respectively. These fields are largely in line with tabulated values and represent a huge improvement relative to a previous attempt to measure g-factors in fission fragments using a cooled Gd/Cf/Gd sandwich in conjunction with the Euroball array<sup>1</sup>. In the previous experiment, no precessions could be measured in either Zr or Mo fragments, which indicated impurity hyperfine fields of less than 1 Tesla for these species. Since there is no reason to expect that the impurity hyperfine fields in other species should not follow tabulated values for implantation into saturated Fe foil, the current data set is likely to provide a large number of new g-factor measurements for low-lying excited states in very neutron-rich nuclei.

\*University of Manchester, United Kingdom, †IREs and Universite Louis Pasteur, Strasbourg, France

<sup>1</sup>A. G. Smith *et al.*, Phys. Lett. **B453**, 206 (1999).

**b.15. Measurements of g-Factors of Excited States in Ba and Ce Nuclei Using Rays from Secondary Fission Fragments** (I. Ahmad, J. P. Greene, A. G. Smith,\* G. S. Simpson,\* J. Billowes,\* P. J. Dagnall,\* J. L. Durell,\* S. J. Freeman,\* M. Leddy,\* W. R. Phillips,\* A. A. Roach,\* J. F. Smith,\* A. Jungclaus,† K. P. Lieb,† C. Teich,† B. J. P. Gall,‡ F. Hoellinger,‡ N. Schulz,‡ and A. Algora§)

An experiment was performed to measure the g-factors of excited states in neutron-rich fission fragments through the time-integral perturbed angular correlation functions between pairs of secondary-fragment rays. The experiment involved the use of a  $^{252}\text{Cf}$  source of total activity 120  $\mu\text{Ci}$  sandwiched between two layers of gadolinium metal. Prior to the deposition of the californium, the gadolinium metal foils (each 20 mg  $\text{cm}^{-2}$  thick) were annealed in an oven at  $650^\circ$  for ten minutes. The magnetization of these foils as a function of temperature and applied field was measured using a magnetometer. The results of this measurement showed that the magnetic moment of the gadolinium reached 87% of its calculated maximum value with the temperature held at 80 K and an applied field of 0.2 T. The californium was then electroplated onto the surface of one of the gadolinium foils and a layer of indium metal (200  $\mu\text{g cm}^{-2}$  thick) was evaporated over a second gadolinium foil. The layer of indium acted as an aid to adhesion between the active foil and the second foil, which was rolled on top to produce a closed source in which the fission fragments stop in gadolinium. The source was placed in a specially designed chamber at the center of the Euroball array. In this chamber the source was clamped between a copper strip and an aluminum plate, the copper strip being attached to a cold copper block that was maintained at 86 K by a constant flow of liquid-nitrogen. A pair of small permanent magnets applying a field of 0.2 T were placed either side of the source in the direction normally reserved for the beam to Euroball. The direction of the applied field could be

reversed by rotating the magnet assembly through an angle of  $180^\circ$ . Even with the rather poor field strengths obtained here, it has proved possible to measure precessions for several states with nanosecond lifetimes. Measurements have been made for the first  $I = 2^+$  states in  $^{144,146}\text{Ba}$  and  $^{146,148}\text{Ce}$ , as well as for the  $9/2^-$  state at 117 keV in  $^{143}\text{Ba}$ , the  $7/2^-$  state at 114 keV in  $^{145}\text{Ba}$  and the yrast  $4^+$  state in  $^{150}\text{Ce}$ . The deduced g-factors are presented in Fig. I-20 and compared with those compiled in reference<sup>1</sup>. It can be seen from this comparison that in general the results obtained here are consistent with previously known g-factors, for those cases where measurements have been made. The measurement of the  $2^+$  state in  $^{146}\text{Ba}$  is consistent with the previous result and provides supporting evidence for a downward trend in the g-factors of the  $2^+$  states of even-even barium isotopes. It has been suggested<sup>2</sup> that this decrease may be explained within the framework of the Interacting Boson Model (IBM2) as due to the increasing number of neutron valence bosons that occurs in the first half of a neutron shell, together with the quenching of the  $Z = 64$  shell gap for  $N > 88$ . Within the IBM2, g-factors for even-even nuclei in this region can easily be calculated following reference<sup>3</sup>, where the g-factors for neutron and proton bosons are taken as  $g = 0.05$  and  $g = 0.63$ . The results of these calculations are shown in Fig. I-20 to give good agreement with the data. The  $^{150}\text{Ce}$  result is the first g-factor measurement in this nucleus and is consistent with the IBM2 predictions. The results of this study were published<sup>4</sup>.

\*University of Manchester, United Kingdom, †University of Göttingen, Germany, ‡IREs and University of Louis Pasteur, Strasbourg, France, §Laboratori Nazionali Legnaro, Italy

<sup>1</sup>P. Raghavan, At. Data Nucl. Data Tables **42**, 189 (1989).

<sup>2</sup>A. Wolf *et al.*, Phys. Lett. **B123**, 165 (1983).

<sup>3</sup>R. L. Gill *et al.*, Phys. Rev. C **33**, 1030 (1986).

<sup>4</sup>A. G. Smith *et al.*, Phys. Lett. **B453**, 206 (1999).

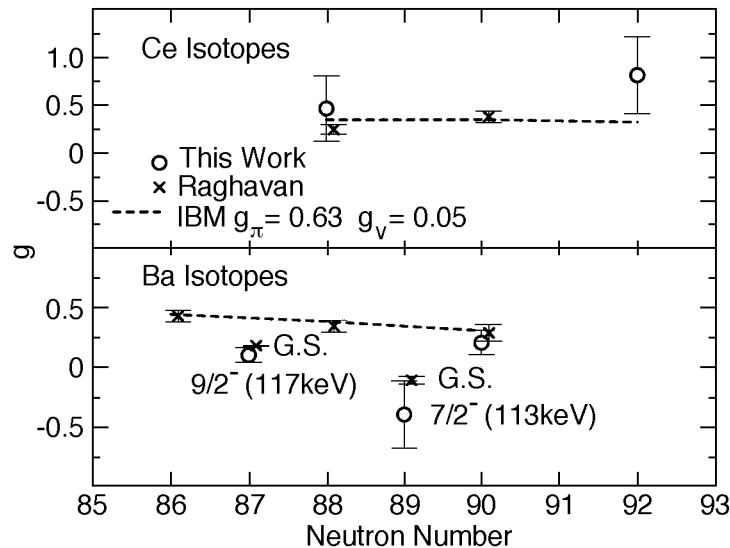


Fig. I-20. The  $g$ -factor results from this work are compared with those compiled in Ref. 1. The first  $2^+$  states in  $^{144}\text{Ba}$  and  $^{148}\text{Ce}$  are used to calibrate the field strengths.

**b.16. In-Beam Gamma-Ray Spectroscopy of the Proton Emitter  $^{131}\text{Eu}$**  (J. J. Ressler,<sup>†</sup> D. Seweryniak,<sup>\*</sup> J. Caggiano, M. P. Carpenter, C. N. Davids, A. Heinz, R. V. F. Janssens, T. L. Khoo, F. G. Kondev, T. Lauritsen, C. J. Lister, P. Reiter, A. A. Sonzogni, J. Uusitalo, Wiedenhöver, P. J. Woods,<sup>‡</sup> W. B. Walters,<sup>†</sup> J. A. Cizewski,<sup>§</sup> B.T. Davinson,<sup>‡</sup> and J. Shergur<sup>†</sup>)

A Recoil-Decay Tagging experiment was carried out to study excited states in the deformed proton emitter  $^{131}\text{Eu}$ . Prompt  $\gamma$  rays were detected using Gammasphere and were tagged with decay protons observed in a Double-Sided Si Strip detector placed behind the focal plane of the Fragment Mass Analyzer. The  $^{58}\text{Ni}(^{78}\text{Kr},p4n)^{131}\text{Eu}$  reaction was used to produce  $^{131}\text{Eu}$  nuclei. Fig. I-21 shows the spectrum of  $\gamma$  rays correlated with the ground-state proton decay in  $^{131}\text{Eu}$ . The spectrum in Fig. I-21 is very complex. At least two rotational bands are present in the spectrum.

However, statistics are too low to observe coincidences between observed  $\gamma$ -ray transitions, and no firm level scheme could be established so far. The data analysis is in progress.

It should be noted that the proton decay to the  $2^+$  excited state in  $^{130}\text{Sm}^1$  was confirmed in the present experiment. In fact, the  $\gamma$ -ray spectrum tagged by the fine structure proton line resembles the spectrum corresponding to the ground-state proton line. This proves that both lines originate from the same state.

<sup>\*</sup>Argonne National Laboratory and University of Maryland, <sup>†</sup>University of Maryland, <sup>‡</sup>University of Edinburgh, United Kingdom, <sup>§</sup>Rutgers University

<sup>1</sup>A. A. Sonzogni *et al.*, Phys. Rev. Lett. **83**, 1116 (1999).

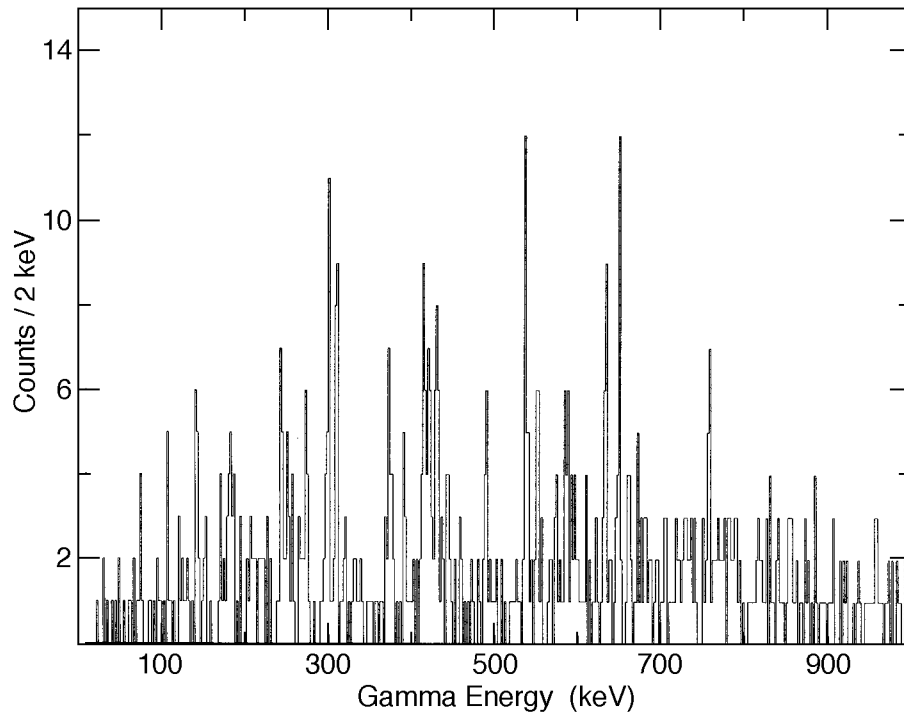


Fig. I-21. The spectrum of  $\gamma$  rays correlated with the ground-state proton decay of  $^{131}\text{Eu}$ .

**b.17. Rotational Bands in the Proton Emitter  $^{141}\text{Ho}$**  (D. Seweryniak,\* J. A. Caggiano, M. P. Carpenter, C. N. Davids, A. Heinz, R. V. F. Janssens, T. L. Khoo, F. G. Kondev, T. Lauritsen, C. J. Lister, P. Reiter, A. A. Sonzogni, J. Uusitalo, I. Wiedenhöver, W. B. Walters,† J. A. Cizewski,§ T. Davinson,‡ K. Y. Ding,§ N. Fotiades,§ U. Garg,¶ J. Shergur,† P. J. Woods,‡ and J. J. Ressler†)

The results of the first in-beam studies of the deformed proton emitter  $^{141}\text{Ho}$  were presented in the previous annual report. A second Recoil-Decay Tagging experiment was carried out to obtain data on excited states in  $^{141}\text{Ho}$  with better statistics. Prompt  $\gamma$  rays were detected using Gammasphere and were tagged with decay protons observed in a Double-Sided Si Strip detector placed behind the focal plane of the Fragment Mass Analyzer. The  $^{54}\text{Fe}(^{92}\text{Mo},p4n)^{141}\text{Ho}$  reaction was used to produce  $^{141}\text{Ho}$  nuclei. Compared to the first experiment inverse kinematics was used this time to narrow the recoil emission cone. As a result about a factor of about 4 more protons were collected and coincidence relationships were established between  $\gamma$  rays observed in the first experiment. Figure I-22 shows the sum of selected  $\gamma$ -ray gates from the ground-state band. As can be seen from Fig. I-22, the ground-state band was extended to spin  $35/2 \hbar$ . In addition,

evidence was found for the unfavored signature partner of the ground-state band.

The dynamic moment of inertia deduced for the ground-state band increases gradually up to the rotational frequency of  $\sim 0.45$  MeV indicating that the alignment of the  $h_{11/2}$  proton pair at  $\sim 0.25$  MeV is blocked. It confirms the  $h_{11/2}$  origin of the ground-state band. Particle-rotor calculations show that the large signature splitting of the ground-state band can be explained only if a significant hexadecapole deformation ( $\epsilon_4 = -0.06$  was calculated by Möller and Nix<sup>1</sup>) and triaxiality is assumed. The  $B(M1)/B(E2)$  ratios deduced for the lower states are also consistent with the  $h_{11/2}$  assignment. The dynamic moment of inertia deduced for the band feeding the isomeric state indicates a band crossing at low rotational frequencies. Since only one signature partner was observed the band has to have a large signature splitting. Among non-

$h_{11/2}$  orbitals near the Fermi surface only the band based on the  $1/2^+[411]$  configuration is expected to have a large signature splitting. The above single-particle assignments are in agreement with the ones proposed based on the proton-decay rates<sup>2</sup>.

In addition to new information on excited states, more precise energy, 1235(9) keV, and half-life, 6.5(-0.7+0.9)  $\mu$ s, was measured for the proton decay from the isomeric state. Despite better statistics, the decay from the ground state and the isomeric state to the  $2^+$  state in  $^{140}\text{Dy}$  was not observed and only an upper limit of 1 % was established for this decay branch.

\*Argonne National Laboratory and University of Maryland, †University of Maryland, ‡University of Edinburgh, United Kingdom, §Rutgers University, ¶University of Notre Dame

<sup>1</sup>P. Möller *et al.*, *At. Nucl. Data Tables* **59**, 185 (1995).

<sup>2</sup>C. N. Davids *et al.*, *Phys. Rev. Lett.* **80**, 1849 (1998).

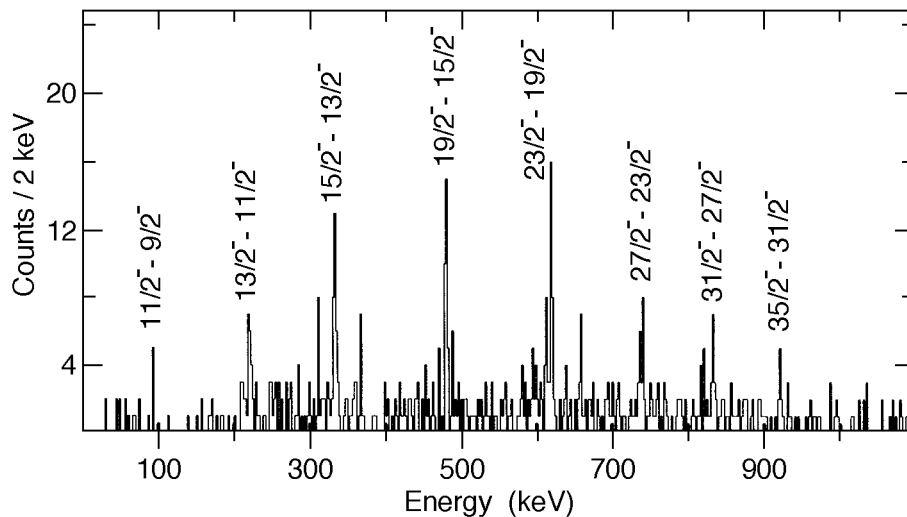


Fig. I-22. The sum of selected  $\gamma$ -ray gates correlated with the ground-state proton decay of  $^{141}\text{Ho}$ .

### b.18. Complex Band Interactions in $^{170}\text{Er}$ (M. P. Carpenter, R. V. F. Janssens, I. Wiedenhöver, C. Y. Wu,\* D. Cline,\* M. W. Simon,\* R. Teng,\* and K. Vetter†)

Two low-lying quadrupole vibrational modes of motion are ascribed to  $\nu_1$  and  $\nu_2$  vibrations. While there is considerable and compelling evidence for the presence of low-lying  $\nu_1$ -vibrational collective excitations, experimental evidence for low-lying  $\nu_2$ -vibrational modes is sparse and often ambiguous. In  $^{170}\text{Er}$  both the  $\nu_1$  and  $\nu_2$  vibrations are located at nearly the same excitation energy, making this nucleus an ideal case to study the  $\nu_2$ -vibrational mode of motion. In addition, low-lying octupole and hexadecapole vibrational bands also have been identified in  $^{170}\text{Er}$ <sup>1</sup>. The closeness in the phonon excitation energies associated with all of these collective modes provides an opportunity to study second-order interactions among them which in turn can help elucidate the validity of collective model descriptions and the microscopic structure underlying these low-lying excitations.

We have recently completed a study of the inelastic excitation of  $^{170}\text{Er}$  targets using a  $^{238}\text{U}$  beam provided by ATLAS. This experiment exploited the combination of the 4 heavy-ion detector array, CHICO<sup>2</sup>, for the kinematics measurement, and Gammasphere for  $\gamma$ -ray detection. In this work, the ground state band was extended to  $26^+$  and the  $\nu_1$ -vibrational band to  $19^+$  ( $K = 2^+$ ). The presumed  $\nu_2$ -vibrational band ( $K = 2^+$ ) and the  $K = 3^+$  were observed up to spin  $22^+$ . Figure I-23 shows the partial level scheme for these four bands deduced from this work. The following observations and conclusions were drawn from the data.

- Strong population of the  $K = 0^+$ ,  $\nu_2$ -vibrational band, brought about by strong mixing with the  $\nu_1$ -vibrational band.
- The  $K = 0^+$  band gains spin alignment faster than the ground band and becomes yrast at

spin  $22^+$  due to strong mixing with the rotationally aligned two-quasiparticle band.

- Appreciable population of the low-lying  $K = 3^+$  hexadecapole vibrational band due to its mixing with the quadrupole  $\nu$ -vibrational band.

the  $\nu$ - and  $\nu$ -vibrational motions and between the quadrupole and hexadecapole vibrational motions ensures that their interactions are of second order in nature and that their collective classification remains justified.

While mixing between the different phonon's does take place, the weakness of the interaction strength between

The results of this study have been recently published in Phys Rev C<sup>3</sup>.

\*University of Rochester, †Lawrence Berkeley National Laboratory

<sup>1</sup>C. M. Baglin, Nucl. Data Sheets **77**, 125 (1996) and references therein.

<sup>2</sup>M. W. Simon *et al.*, Nucl. Instrum. Methods Phys. Res. A (to be published).

<sup>3</sup>C. Y. Wu *et al.*, Phys Rev C **61**, 021305(R) (2000).

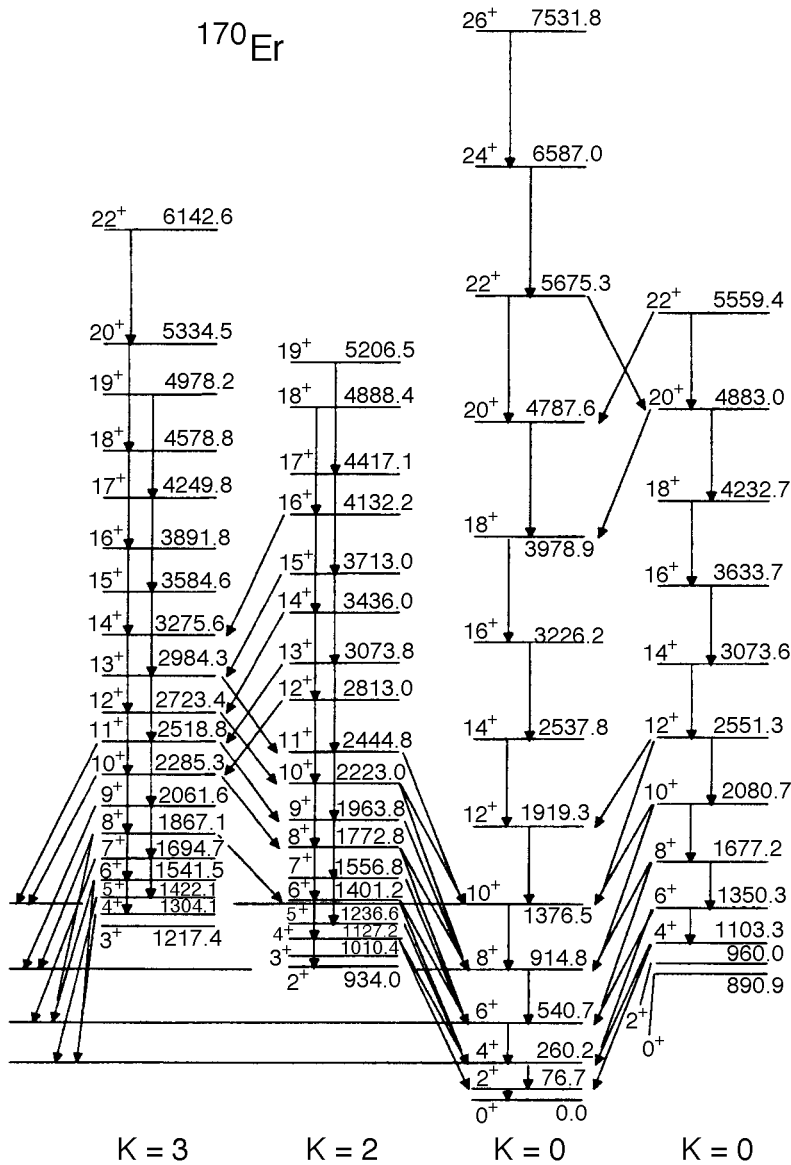


Fig. I-23. Partial level scheme of the  $K = 3$ ,  $\nu$ -vibrational, ground-state, and  $\nu$ -vibrational bands for  $^{170}\text{Er}$ .

**b.19. Entry Distributions and Fusion Dynamics in the Radiative Capture Reaction of  $^{90}\text{Zr} + ^{90}\text{Zr}$**  (M. P. Carpenter, K. Abu Saleem, I. Ahmad, J. Caggiano, C. N. Davids, A. Heinz, R. V. F. Janssens, R. A. Kaye, T. L. Khoo, F. G. Kondev, T. Lauritsen, C. J. Lister, J. Ressler, D. Seweryniak, A. A. Sonzogni, I. Wiedenhöver, S. Siem,\* B. Heskind,‡ H. Amro,† W. C. Ma,‡ W. Reviol,§ L. L. Riedinger,¶ D. G. Sarantites,§ and P. G. Varmette†)

Some years ago, the surprising observation of fusion without subsequent particle evaporation was reported for the  $^{90}\text{Zr} + ^{90}\text{Zr}$  system at the Coulomb barrier<sup>1,2</sup>. The process was found to have cross sections as high as  $\sim 40 \mu\text{b}$ .

An experiment dedicated to a further study of radiative capture in the  $^{90}\text{Zr} + ^{90}\text{Zr}$  system was recently performed at the ATLAS facility with Gammasphere and the Fragment Mass Analyzer (FMA). With the calorimetric capabilities of the spectrometer and the selectivity of the FMA, it was possible to investigate in detail the gamma decay of  $^{180}\text{Hg}$  using the recoil decay tagging (RDT) technique for channel selection.

In such measurements, the isotopic purity of the target is an important consideration given the much stronger cross sections for evaporation channels. For this reason, measurements were performed not only with a  $^{90}\text{Zr}$  target, but also with  $^{91}\text{Zr}$  and  $^{92}\text{Zr}$  targets. For all

projectile-target combinations, the properties of the various reaction channels were investigated at beam energies ranging from 369 up to 410 MeV.

By utilizing the RDT technique, spectra for the  $\gamma$ -ray total energy and multiplicity were produced for the capture channel,  $^{180}\text{Hg}$ . In both cases, the distributions were wider than the corresponding spectra for the evaporation channels. This is due to the fact that our  $^{90}\text{Zr}$  target is not isotopically pure, allowing  $^{180}\text{Hg}$  to be produced in reactions involving the impurities  $^{91}\text{Zr}$  and  $^{92}\text{Zr}$ . However, when the contribution of these impurities are subtracted from each spectrum, the resulting distributions in total energy and multiplicity lie at higher excitation energy and multiplicity than those distributions associated with evaporation channels. This clearly shows that the capture channel is produced at the highest excitation energies and angular momentum produced by the reaction.

\*Argonne National Laboratory and University of Oslo, Norway, †Mississippi State University, ‡Niels Bohr Institute, Roskilde, Denmark, §Washington University, ¶University of Tennessee

<sup>1</sup>J. G. Keller *et al.*, Nucl. Phys. **A452**, 173 (1986).

<sup>2</sup>K.-H. Schmidt *et al.*, Phys. Lett. **B168**, 39 (1986).

- b.20. First Observation of Excited Structures in Neutron Deficient, Odd-Mass Pt, Au and Hg Nuclei** (F. G. Kondev, K. Abu Saleem, I. Ahmad, M. Alcorta, P. Bhattacharyya, L. T. Brown, J. Caggiano, M. P. Carpenter, C. N. Davids, S. M. Fischer, A. Heinz, R. V. F. Janssens, R. A. Kaye, T. L. Khoo, T. Lauritsen, C. J. Lister, G. L. Poli, J. Ressler, D. Seweryniak, A. A. Sonzogni, I. Wiedenhöver, H. Amro,\* S. Siem,† J. Uusitalo,‡ J. A. Cizewski,§ M. Danchev,¶ D. J. Hartley,¶ B. Heskind,|| W. C. Ma,\*\* R. Nouicer,†† W. Reviol,‡‡ L. L. Riedinger,¶¶ M. B. Smith,§ and P. G. Varmette\*\*)

The neutron deficient nuclei near  $Z = 82$  play a seminal role in elucidating the contributions of various orbitals to the many different nuclear shapes seen in this mass region. The microscopic understanding of the excited prolate structures discovered recently in the near drip line isotopes  $^{176}\text{Hg}$  and  $^{178}\text{Hg}$ <sup>1,2,3</sup> requires spectroscopic knowledge of the level structures in neighboring odd-mass Hg and Au nuclei as the latter provide the possibility to isolate the shape driving effects of individual orbitals.

A number of dedicated experiments have been performed at ATLAS using Gammasphere in conjunction with the recoil-decay tagging technique. By combining the simplicity of  $\gamma$ -decay spectroscopy following mass selection with the complexity of in-beam  $\gamma$ -ray coincidence techniques, comprehensive level schemes of many neutron deficient isotopes were established for the first time. Among these are:  $^{173}\text{Pt}$ ,  $^{173-177}\text{Au}$  and  $^{175-179}\text{Hg}$ . In addition, we have significantly extended the previously known level schemes of  $^{174-176}\text{Pt}$ . Special attention was devoted to

level structures built upon the intruder  $h_{9/2}$  and  $i_{13/2}$  proton orbitals, as well as to those associated with the  $p_{3/2}$  and  $i_{13/2}$  neutron configurations. A sample  $\gamma$ -ray spectrum showing  $\gamma$  rays associated with the  $1/2^- [521]$  ( $p_{3/2}$ ) band in  $^{179}\text{Hg}$  is presented in Fig. I-24. Surprisingly, the odd-mass, neutron-deficient Au and Hg isotopes exhibit persistent collectivity at relatively low excitation energy. This should be contrasted with the rapid rise of the excitation energy of the prolate band for the  $N < 100$  even-even Hg neighbors. In addition to the in-beam spectroscopy studies, we have also performed a detailed investigation of the  $\alpha$ -decay properties of these isotopes. We have revised many of the decay schemes and this provides for a better understanding of the structure of these nuclei. Alpha energy spectra showing the main decays of  $^{177}\text{Au}$  and its daughter isotope  $^{173}\text{Ir}$  are presented in Fig. I-25. Sample spectra of  $\gamma$  rays in coincidence with selected  $^{174}\text{Au}$  lines are shown in Fig. I-26.

The analysis of the data is still in progress.

\*Argonne National Laboratory and Mississippi State University, †Argonne National Laboratory and University of Oslo, Norway, ‡Argonne National Laboratory and University of Jyväskylä, Finland, §Rutgers University, ¶University of Tennessee, ||The Niels Bohr Institute, Roskilde, Denmark, \*\*Mississippi State University, ††University of Illinois at Chicago, ‡‡Washington University

<sup>1</sup>M. P. Carpenter *et al.*, Phys. Rev. Lett. **78**, 3650 (1997).

<sup>2</sup>M. Muikku *et al.*, Phys. Rev. C **58**, R3033 (1998).

<sup>3</sup>F. G. Kondev *et al.*, Phys. Rev. C **61**, 011303(R) (2000).

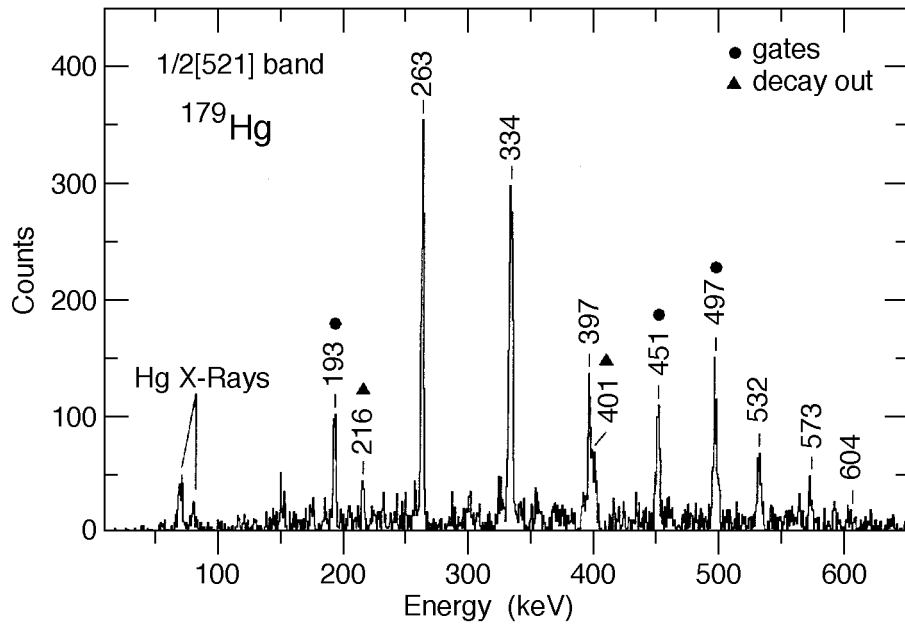


Fig. I-24. Sample spectrum obtained from the mass-gated coincidence data for the  $1/2^- [521] (p_{3/2})$  band observed in  $^{179}\text{Hg}$ . The spectrum is the result of sums of coincidence gates placed on the transitions marked with the black dots.

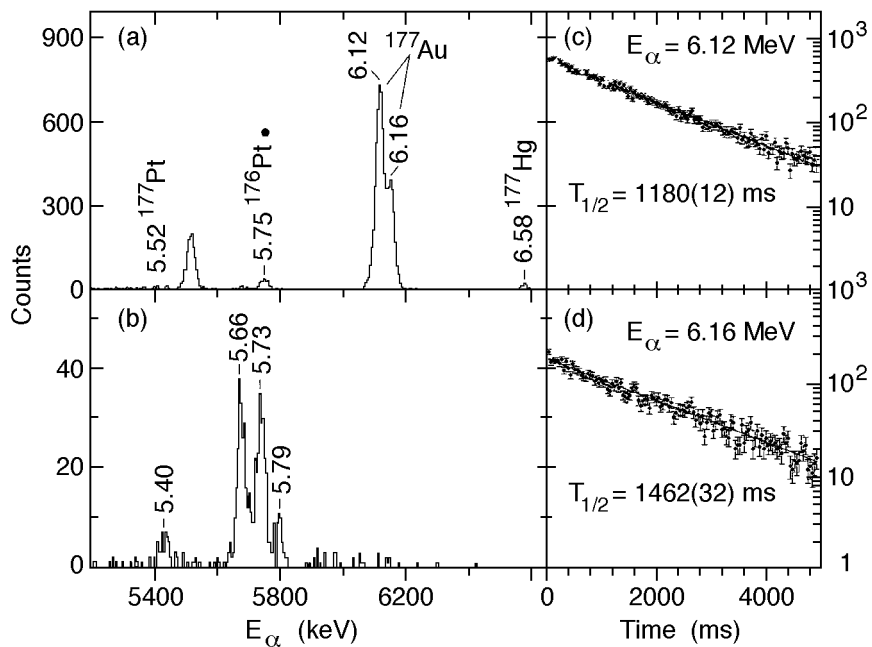


Fig. I-25(a). First generation  $\alpha$ -energy spectrum for  $A = 177$  selected recoils. (Note, that the presence of the 5.75 MeV line of  $^{176}\text{Pt}$  is due to the subsequent  $\beta^+$  decay of  $^{177}\text{Au}$ .) (b) Second generation  $\alpha$ -energy spectrum correlated with the  $E_\alpha = 6.12$  MeV line. Time decay spectra for the  $E_\alpha = 6.12$  MeV (c) and 6.16 MeV (d) lines. The fitted curves are shown with solid lines.

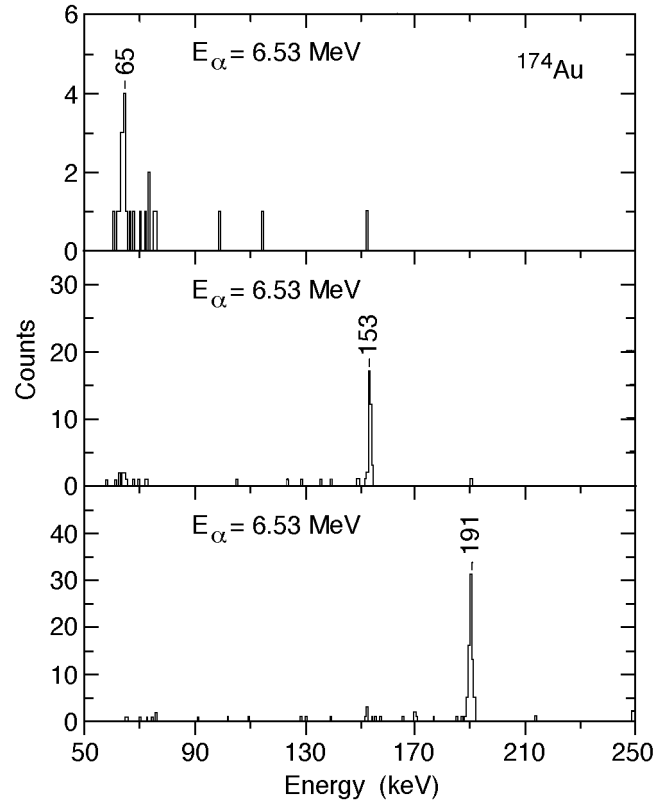


Fig. I-26. Spectra of  $\gamma$ -rays in coincidence with the  $^{174}\text{Au}$  characteristics  $\alpha$ -lines.

**b.21. Spectroscopy of Neutron Deficient Even-Even Hg Nuclei** (F. G. Kondev, K. Abu Saleem, I. Ahmad, M. Alcorta, P. Bhattacharyya, L. T. Brown, J. Caggiano, M. P. Carpenter, C. N. Davids, S. M. Fischer, A. Heinz, R. V. F. Janssens, R. A. Kaye, T. L. Khoo, T. Lauritsen, C. J. Lister, J. Ressler, D. Seweryniak, A. A. Sonzogni, I. Wiedenhöver, H. Amro,\* S. Siem,† J. Uusitalo,‡ B. Heskind,§ W. C. Ma,¶ R. Nouicer,|| W. Reviol,\*\* L. L. Riedinger,†† and P. G. Varmette¶)

Neutron deficient Hg nuclei are characterized by level structures associated with prolate and oblate deformations. The prolate bands find their origin in multi-particle-hole excitations across the  $Z = 82$  shell gap involving several proton intruder orbitals<sup>1,2</sup>. Mean field calculations by Nazarewicz<sup>3</sup> predict that the prolate minimum for Hg and Pb isotopes with  $N < 98$  evolves towards much larger deformations ( $\beta \sim 0.50-0.56$ ), but its excitation energy rises up to  $\sim 3.5$  MeV. Nuclei in this region also exhibit a variety of collective excitations. For example, due to the presence of pairs of orbitals with  $j = l = 3 \hbar$  near both the proton and neutron Fermi surfaces, octupole vibrations should be enhanced at low spin. Such structures will compete along the yrast line with collective excitations built on specific quasiparticle configurations. This situation provides an opportunity to study the interplay between these collective modes.

In last year's Annual Report a study was reported of yrast structures in  $^{178}\text{Hg}$ , as a part of our program to investigate properties of very neutron deficient Hg nuclei in this region. The level scheme for this nucleus,

deduced from this work, is presented in Fig. I-27 and its investigation has now been completed<sup>4</sup>. At the ATLAS facility, we have investigated this year the  $^{180}\text{Hg}$  isotope, which was produced as a by-product of an experiment dedicated to the study of fusion dynamics in the vicinity of the Coulomb barrier. A sample  $\gamma$ -ray spectrum showing the main transitions in  $^{180}\text{Hg}$  is presented in Fig. I-28. Particular attention was paid to the low-lying negative parity excitations which have been observed for the first time in  $^{178}\text{Hg}$  and  $^{180}\text{Hg}$ . They exhibit a complex decay towards the low spin states arising from both the prolate-deformed and the nearly spherical coexisting minima. These structures are associated at low spin with an octupole vibration and are crossed at moderate frequency by shape driving, two-quasiproton excitations. Striking similarities are noted and a consistent interpretation appears to emerge based on detailed comparisons with various model calculations.

A brief account of the data on the  $^{178}\text{Hg}$  nucleus has been published<sup>4</sup> and a full report on  $^{180}\text{Hg}$  has been submitted for publication.

\*Argonne National Laboratory and Mississippi State University, †Argonne National Laboratory and University of Oslo, Norway, ‡Argonne National Laboratory and University of Jyväskylä, Finland, §The Niels Bohr Institute, Roskilde, Denmark, ¶Mississippi State University, ||University of Illinois at Chicago, \*\*Washington University, ††University of Tennessee

<sup>1</sup>J. L. Wood, K. Heyde, W. Nazarewicz, M. Huyse, and P. Van Duppen, Phys. Rep. **215**, 103 (1992).

<sup>2</sup>K. Heyde, P. Van Isacker, M. Waroquier, J. L. Wood, and R. A. Meyer, Phys. Rep. **102**, 293 (1983).

<sup>3</sup>W. Nazarewicz, Phys. Lett. **B305**, 195 (1993).

<sup>4</sup>F. G. Kondev *et al.*, Phys. Rev. C **61**, 011303(R) (2000).

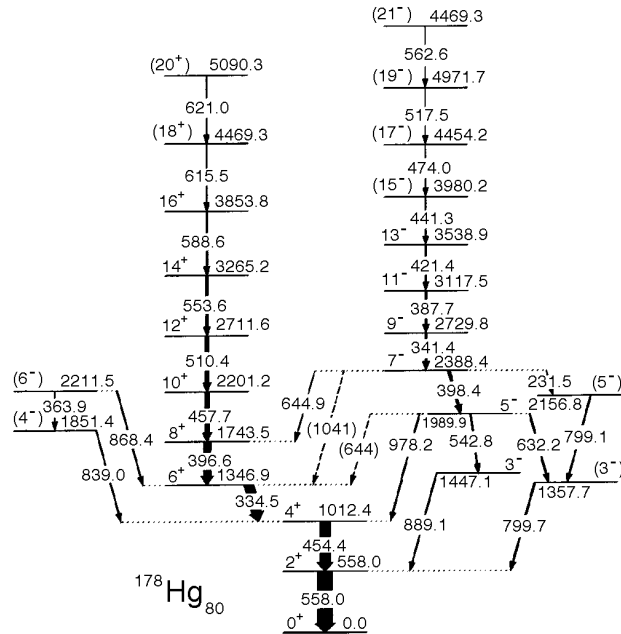


Fig. I-27. Proposed  $^{178}\text{Hg}$  level scheme. Quantum numbers are given in parenthesis when reliable multipolarity information was not obtained. For each transition, the width of the arrow is proportional to the measured intensity.

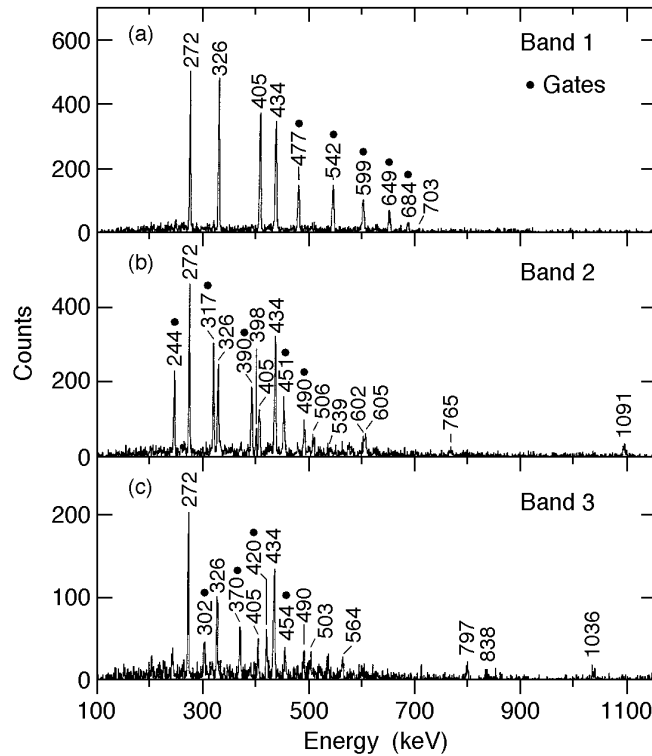


Fig. I-28. Sample spectra obtained from the mass-gated coincidence data for bands observed in  $^{180}\text{Hg}$ . The spectra are sums of coincidence gates placed on the transitions marked with the black dots.

**b.22. High-Spin Collective Structures in  $^{178}\text{Pt}$**  (F. G. Kondev, M. Alcorta, P. Bhattacharyya, L. T. Brown, M. P. Carpenter, C. N. Davids, S. M. Fischer, R. V. F. Janssens, T. L. Khoo, T. Lauritsen, C. J. Lister, D. Seweryniak, A. A. Sonzogni, I. Wiedenhöver, S. Siem,<sup>\*</sup> J. Uusitalo,<sup>†</sup> R. Nouicer,<sup>‡</sup> W. Reviol,<sup>§</sup> and L. L. Riedinger<sup>¶</sup>)

Despite their close proximity to the  $Z = 82$  shell closure, the Pt ( $Z = 78$ ) nuclei of the  $A \sim 180$  region are characterized by level structures associated with prolate, oblate and triaxial deformations. In these nuclei, excitations based on the intruder orbitals have received considerable attention because of their ability to affect the nuclear shape. While in the Os ( $Z = 76$ ) nuclei the quadrupole deformation is approximately constant over a wide range of isotopes, there is evidence in the Hg ( $Z = 80$ ) isotopes that structures built upon specific intruder orbitals impact the nuclear shape significantly. Specifically, Ma *et al.*<sup>1</sup> have shown in  $^{186}\text{Hg}$  that the occupation of the  $1/2^+[651]$  ( $g_{9/2}$ ) and  $1/2^- [770]$  ( $j_{15/2}$ ) neutron orbitals drives the nucleus towards a prolate deformation value of  $\beta \sim 0.35$  which is intermediate between those associated with the normally deformed ( $\beta \sim 0.25$ ) and the superdeformed ( $\beta \sim 0.50$ ) minima. In this general context the study of Pt nuclei is worthwhile as it is likely to add information on the relative importance of various orbitals for the collective excitations in this mass region.

Excited states in  $^{178}\text{Pt}$  were populated with the  $^{103}\text{Rh}(^{78}\text{Kr},3p)$  reaction using 350-MeV beams provided by the ATLAS superconducting linear accelerator at the Argonne National Laboratory. An extended level scheme for  $^{178}\text{Pt}$ , shown in Fig. I-29,

was obtained by combining the selectivity of the FMA with the high detection efficiency and resolving power of the Gammasphere spectrometer. Specifically, the ground state band was observed beyond the first crossing which is attributed to the alignment of a pair of  $i_{13/2}$  neutrons. The previously known excited band was firmly assigned odd-spin and negative parity, and was considerably extended in spin. A new negative parity band was observed for the first time. The configurations of these structures were interpreted as octupole vibrations at low spin which are crossed at higher frequency by two-quasiparticle excitations. The latter are most likely neutron excitations. Such assignments were aided by examining a range of properties including (a) the excitation energy of the bands, (b) the E1 transition probabilities and (c) alignments (see Fig. I-30). In addition, the  $\beta^-$ -decay reduced widths for the Pt isotopes were also investigated. The large reduction of the width for the odd-mass Pt isotopes is explained through the weakening of neutron pairing due to the blocking effect. As illustrated in Fig. I-31, such a behavior is reproduced by blocked Nilsson-Lipkin-Nogami calculations.

A full report of this work has been accepted for publication.

<sup>\*</sup>Argonne National Laboratory and University of Oslo, Norway, <sup>†</sup>Argonne National Laboratory and University of Jyväskylä, Finland, <sup>‡</sup>University of Illinois at Chicago, <sup>§</sup>Washington University, <sup>¶</sup>University of Tennessee  
<sup>1</sup>W. C. Ma *et al.*, Phys. Rev. C **47**, R5 (1993).

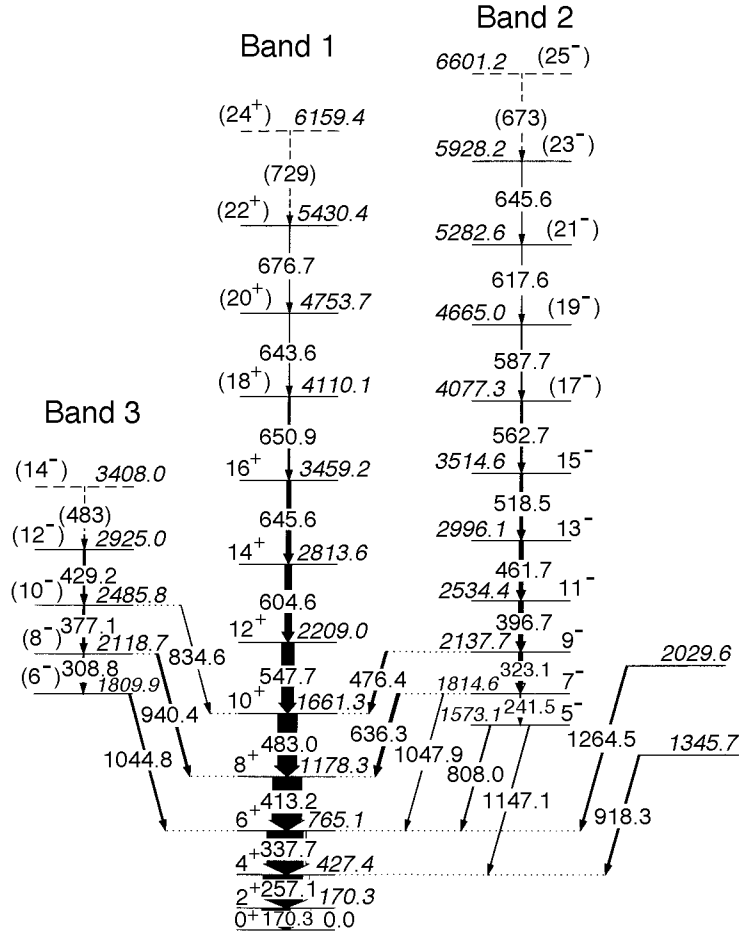


Fig. I-29. Level scheme of  $^{178}\text{Pt}$  deduced from this work. Tentative placements are indicated by dashed lines. Tentative spin-parity assignments are given in brackets.

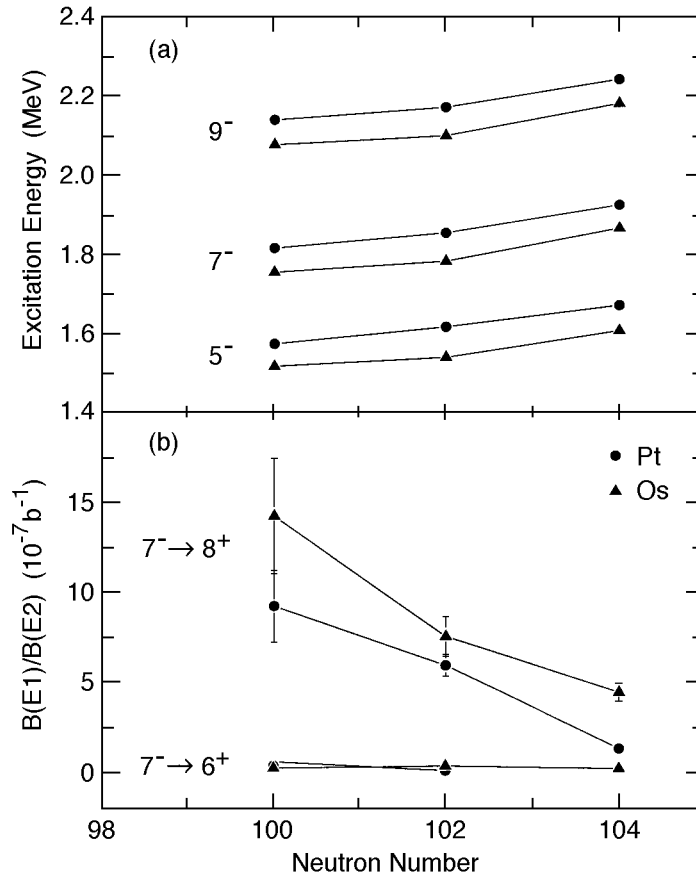


Fig. 1-30. Excitation energies for the 5<sup>-</sup>, 7<sup>-</sup> and 9<sup>-</sup> levels (a) and B(E1)/B(E2) ratios for selected transitions (b) in <sup>178</sup>Pt and neighboring even-even Os and Pt isotopes.

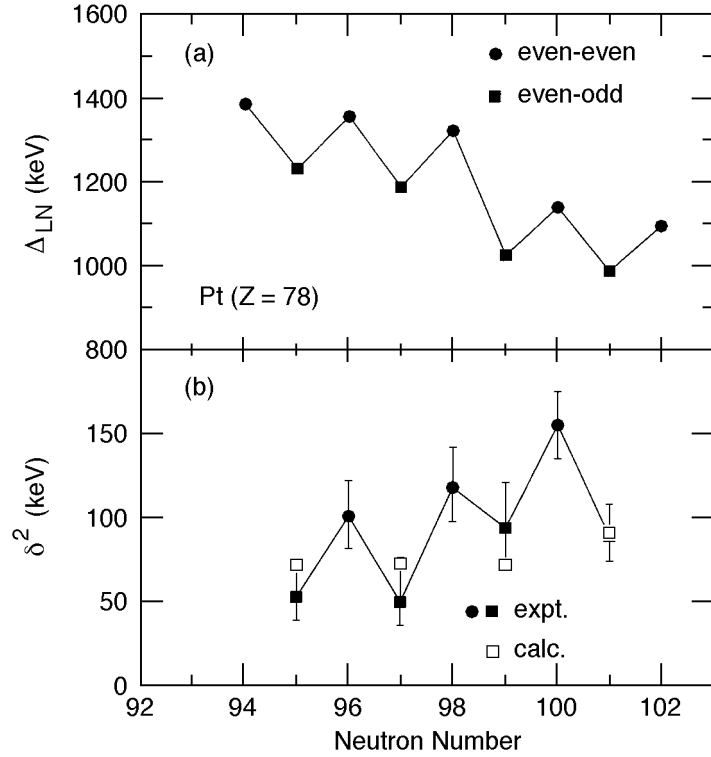


Fig. I-31. (a) Calculated Lipkin-Nogami pairing gap parameter  $\Delta_{LN}$  for selected even-even and odd-A Pt isotopes. (b) Experimental (filled symbols) and calculated (open symbols)  $\alpha$ -decay reduced widths for several Pt isotopes. The calculated  $\delta^2$  values were deduced from the predicted  $F$  values and the experimental data for the reduced widths of the even-even neighboring nuclei (see the text for details).

**b.23. Spectroscopy of  $^{183}\text{Tl}$  with Recoil-Mass and Z Identification** (M. P. Carpenter, R. V. F. Janssens, T. Lauritsen, D. Seweryniak, J. Uusitalo, I. Wiedenhöver, W. Reviol,\* D. Jenkins,† K. S. Toth,‡ C. R. Bingham,\* L. L. Riedinger,\* W. Weintraub,\* J. Cizewski,§ R. Wadsworth,† A. N. Wilson,† C. J. Gross,‡¶ J. C. Batchelder,¶ S. Juutinen,|| and K. Helariutta||)

The spectroscopy of  $^{183}\text{Tl}$  has been the focus of an experiment with Gammasphere coupled to the FMA. The  $^{182,183}\text{Tl}$  nuclei have also been studied as byproducts of a search for  $^{182}\text{Pb}$  at RITU in Jyväskylä<sup>1</sup>. In these two experiments, the yrast sequence in  $^{183}\text{Tl}$  has been observed for the first time (see Fig. I-32). The results reported here and in Ref. 2 are mainly based on the spectroscopy of  $^{183}\text{Tl}$  with mass identification. The identified yrast sequence in  $^{183}\text{Tl}$  resembles the well-deformed (prolate) excited bands in adjacent nuclei of Hg, Tl, and Pb, but its decay-out properties are different from those cases in two respects. (i) The rotational-like sequence is observed from medium spin to the  $13/2^+$  state, *i.e.* the

population intensity stays within the band down to the bandhead. (ii) A strong  $\gamma$ -decay branch from the prolate band to a slightly-oblate structure, like in heavier Tl nuclei, is not observed. These features suggest that the prolate energy minimum in  $^{183}\text{Tl}$  has dropped significantly compared to  $^{185}\text{Tl}$ <sup>3</sup>. In the present level scheme it is not clear how the  $^{183}\text{Tl}$  band decays and, therefore, upper and lower-limit estimates for the energy of the  $13/2^+$  bandhead relative to the  $9/2^-$  isomeric state (oblate) have been made (95 keV  $E_{rel}$  424 keV<sup>2</sup>). However, with the estimated upper limit, the basic conclusions for the  $i_{13/2}$  band in  $^{183}\text{Tl}$  are not affected by the uncertainty for the decay out of the band.

\*University of Tennessee, †University of York, United Kingdom, ‡Oak Ridge National Laboratory, §Rutgers University, ¶Oak Ridge Associated Universities, ||University of Jyväskylä, Finland

<sup>1</sup>D. Jenkins, *et al.*, to be published.

<sup>2</sup>W. Reviol *et al.*, Proceedings of the Conference “Nuclear Structure ‘98”, Gatlinburg, TN, AIP-Conference Proceedings, in print.

<sup>3</sup>G. Lane *et al.*, Nucl. Phys. **A586**, 316 (1995).

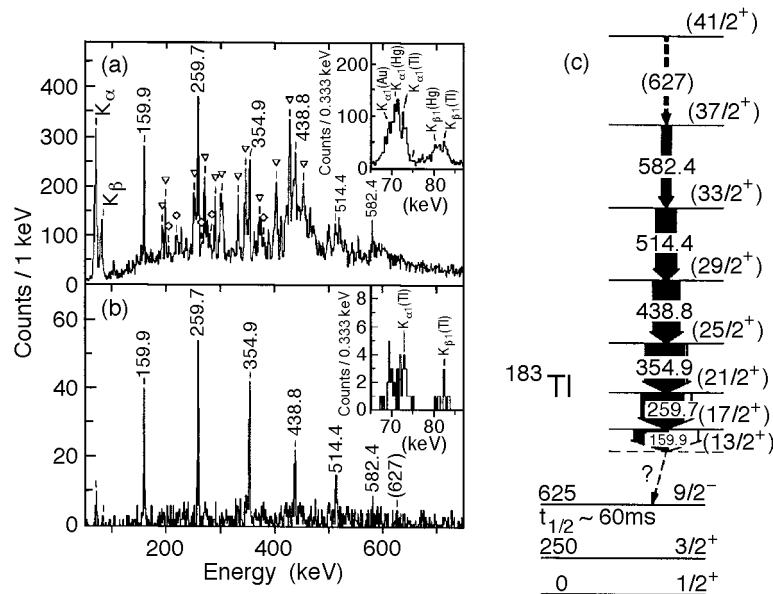


Fig. I-32. (a) Gamma rays in coincidence with  $A = 183$  residues. Known transitions in  $^{183}\text{Hg}$  and  $^{183}\text{Au}$  are labeled by triangles and diamonds. Newly observed transitions are labeled by their energies in keV. (b) Summed spectrum of gates on the 159.9-, 259.7-, 354.9-, 438.8-, and 514.4-keV lines from the  $A = 183$   $E^-E$  coincidence data. (c) Deduced level structure for  $^{183}\text{Tl}$ .

**b.24. Identification of a  $t_{1/2} > 1$  ms K-Isomer in Neutron-Rich  $^{185}\text{Ta}$**  (I. Ahmad, M. P. Carpenter, G. Hackman, R. V. F. Janssens, T. L. Khoo, D. Nisius, P. Reiter, C. Wheldon,\* P. M. Walker,\* R. D'Alarcao,† P. Chowdhury,† C. J. Pearson,\* E. H. Seabury,† and D. M. Cullen‡)

Our program of using pulsed heavy beams to populate long-lived high- $K$  isomers in neutron-rich nuclei in the  $A \approx 180$  region has proven to be extremely successful. Experiments with U beams on Lu, Hf, Ta and W isotopes have yielded many new multi-quasiparticle isomers, overcoming the limitations of fusion-evaporation reactions in reaching the neutron-rich nuclei in this region. The results of the strongest reaction channels have been published<sup>1,2</sup>, and we are now making progress on the weaker channels involving nucleon transfer. Here we report on a new long-lived isomer in neutron-rich  $^{185}\text{Ta}$ , populated via 1-proton transfer with a 1600 MeV pulsed  $^{238}\text{U}$  beam incident on a thick target of  $^{186}\text{W}$ . The  $\gamma$  rays were measured by the ANL/Notre-Dame BGO array.

The out-of-beam spectra are dominated by the strong inelastic excitation of  $K$  isomers in the target nucleus<sup>1</sup>. However, a new band has been observed from the particle transfer channels, (see Fig. I-33) fed by a  $t_{1/2} > 1$  ms isomer. The population intensity and careful analysis of the weak x-ray coincidences suggest that the new band is in the isotope  $^{185}\text{Ta}$  (1-proton from the target). An earlier (t,  $\gamma$ ) experiment<sup>3</sup> identified 3 low-lying states in the  $K = 9/2$  band in  $^{185}\text{Ta}$ , the energies of which are in excellent agreement with the

corresponding levels in the new band. In addition, intensity balancing arguments have been used to extract an electron conversion coefficient for the 175 keV transition, leading to an E1 assignment. This is consistent with a  $K$ -allowed decay from the  $K = 9/2^-$  bandhead to the  $K = 7/2^-$  ground state, and is also of approximately the right energy to continue the systematics observed in the lighter isotopes. Examination of the in-band  $\gamma$ -ray branching ratios supports the  $9/2^- [514]$  Nilsson configuration assignment.

Adding one unit of spin for each level above an  $I = 9/2^-$  bandhead would mean that the transition directly de-populating the isomer feeds the  $19/2^-$  member of the band (see Fig. I-33 inset for proposed level scheme). This transition has not been observed but can be given upper energy limits of 100 keV (M1) and 80 keV (E1) on the basis of detection-efficiency and conversion-coefficient considerations. Comparison with Nilsson model calculations favors a  $K = 21/2^- \{5/2^- [402], 7/2^+ [404], 9/2^- [514]\}$  3-quasiproton configuration for the isomer, consistent with an isomeric M1 transition. This is the most neutron-rich seniority  $> 2$   $K$ -isomer identified and the results have been published<sup>4</sup>.

\*University of Surrey, United Kingdom, †University of Massachusetts, ‡University of Liverpool, United Kingdom

<sup>1</sup>C. Wheldon *et al.*, Phys. Lett. **B425**, 239 (1998).

<sup>2</sup>R. D'Alarcao *et al.*, Phys. Rev. C **59**, R1227 (1999).

<sup>3</sup>G. Lovhoiden, D. G. Burke, E. R. Flynn, and J. W. Sunier, Phys. Scr. **22**, 203 (1980).

<sup>4</sup>C. Wheldon *et al.*, Eur. Phys. J. **A5**, 353 (1999).

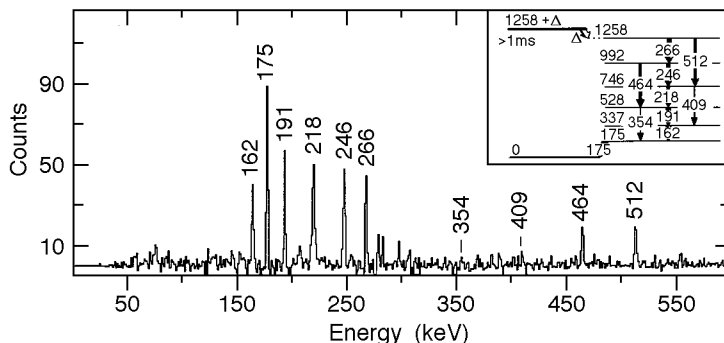


Fig. I-33. The gamma-ray spectrum gated on transitions in the new band. A level scheme is proposed (see inset panel), with a well formed rotational structure being fed by an isomeric state. The low energy isomeric transition has not been observed leading to an offset of triangle for the isomeric level.

**b.25. Studies of the Excited States and the Decay of  $^{185}\text{Bi}$**  (G. L. Poli, D. Seweryniak,\* M. P. Carpenter, C. N. Davids, A. Heinz, R. V. F. Janssens, T. L. Khoo, F. G. Kondev, A. A. Sonzogni, I. Wiedenhöver, P. J. Woods,† T. Davinson,† J. A. Cizewski,§ J. J. Ressler,‡ J. Shergur,‡ and W. B. Walters‡)

A Recoil-Decay Tagging experiment was carried out to study the proton decay and excited states of  $^{185}\text{Bi}$ . Prompt  $\gamma$  rays were detected using Gammasphere and were tagged with decay protons observed in a Double-Sided Si Strip detector placed behind the focal plane of the Fragment Mass Analyzer. The  $^{96}\text{Mo}(^{92}\text{Mo},p2n)^{185}\text{Bi}$  reaction was used to produce  $^{185}\text{Bi}$  nuclei. The decay spectrum is shown in Fig. I-34. Compared to the first discovery experiment<sup>1</sup> a

factor of about 4 more protons and  $\gamma$  particles associated with  $^{185}\text{Bi}$  were detected. An energy of 1618(11) keV and a half-life of  $50_{(-9)}^{(+7)} \mu\text{s}$  was obtained for the decay of  $^{185}\text{Bi}$ . An energy of 1618(11) keV was measured for the protons and 8080(30) keV for the  $\alpha$  particles. The proton-decay branching ratio was deduced to be 85%. The analysis of  $\gamma$ -ray data is in progress.

\*Argonne National Laboratory and University of Maryland, †University of Edinburgh, United Kingdom,

‡University of Maryland, §Rutgers University

<sup>1</sup>C. N. Davids *et al.*, Phys. Rev. Lett. **76**, 592 (1995).

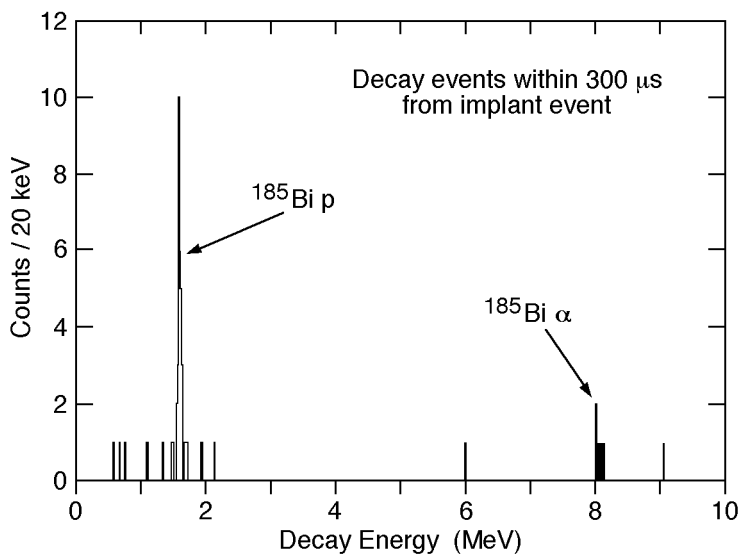


Fig. I-34. The decay spectrum associated with  $^{185}\text{Bi}$ .

**b.26. Coulomb Excitation and Few Nucleon Transfer Reactions for the  $^{209}\text{Bi} + ^{232}\text{Th}$  System** (R. V. F. Janssens, I. Ahmad, J. Caggiano, M. P. Carpenter, J. P. Greene, A. Heinz, T. L. Khoo, F. G. Kondev, T. Lauritsen, C. J. Lister, D. Seweryniak, A. Sonzogni, I. Wiedenhoever, H. Amro,\* K. Abu Saleem,† G. Hackman,‡ P. Chowdhury,§ D. Cline,¶ A. O. Machiavelli,| and C. Wu¶)

For the past two years, we have studied the high-spin collective behavior of long-lived actinide nuclei with the so-called "unsafe" Coulomb excitation technique with DC beams of very heavy ions at energies a few % above the Coulomb barrier and multi-detector arrays with a large number of Compton-suppressed Ge detectors. Some of this work has been published<sup>1,2</sup>, while other parts are described elsewhere in this report. From the perspective of extending the "unsafe" Coulex technique, a tantalizing result was the observation and isotopic assignment of bands populated in transfer reactions. For example, in our study of the  $^{208}\text{Pb} + ^{244}\text{Pu}$  reaction, two new rotational cascades were assigned to the yrast band of  $^{243}\text{Pu}$  from cross-coincidence relationships with transitions in  $^{209}\text{Pb}$ . Such a transfer reaction was subsequently used to gather data on  $^{238}\text{Pu}$  with the  $^{207}\text{Pb} + ^{239}\text{Pu}$  reaction at 1300 MeV. The choice of the odd-neutron  $^{207}\text{Pb}$  projectile was determined by the desire to enhance neutron pick-up from the target.

The success encountered in these measurements led to the suggestion that exciting possibilities might exist to use proton transfer channels to study high-Z nuclei beyond Pu and Cm by using the appropriate projectile, e.g.  $^{209}\text{Bi}$ . The  $^{209}\text{Bi} + ^{232}\text{Th}$  reaction at 1400 MeV was studied at ATLAS with the Gammasphere

spectrometer in order to answer the following questions: (1) how large are the cross sections for proton transfers, compared to Coulex? (2) how many reaction channels are actually open? (3) how large is the angular momentum transfer? (4) what types of excitations are observable? (5) are more complex reactions corresponding to the transfer of large number of nucleons observed?

While the data are still under analysis, the following general conclusions have already been reached: (i) One proton transfer and pick-up reactions to  $^{233}\text{Pa}$  and  $^{231}\text{Ac}$  have been observed with a yield of  $\sim 5\%$  with respect to the intensity of  $^{232}\text{Th}$ . This yield is comparable to that seen in the neutron transfer channels on the Pu targets. (ii) The yield for the two-proton transfer channel is lower by roughly one order of magnitude, again in line with expectations. (iii) States with spins as high as  $\sim 25_{-}$  have been observed. (iv) In addition to proton transfer, the neutron channels to  $^{233,231,230}\text{Th}$  have also been observed. The intensities and spins reached are similar to those of the proton channels. Figure I-35 presents partial levels schemes obtained for  $^{231}\text{Ac}$  and  $^{233}\text{Pa}$ . The level scheme of  $^{232}\text{Th}$  was considerably extended as well. The latter will be combined with results obtained in a similar experiment at the 8PI spectrometer<sup>3</sup>.

\*Argonne National Laboratory and North Carolina State University, †Argonne National Laboratory and Illinois Institute of Technology, ‡University of Kansas, §University of Massachusetts-Lowell, ¶University of Rochester, |Lawrence Berkeley National Laboratory

<sup>1</sup>G. Hackman *et al.*, Phys. Rev. C **57**, R1506 (1998).

<sup>2</sup>I. Wiedenhoever *et al.*, Phys. Rev. Lett. **83**, 2143 (1999).

<sup>3</sup>D. Ward *et al.*, private communication.

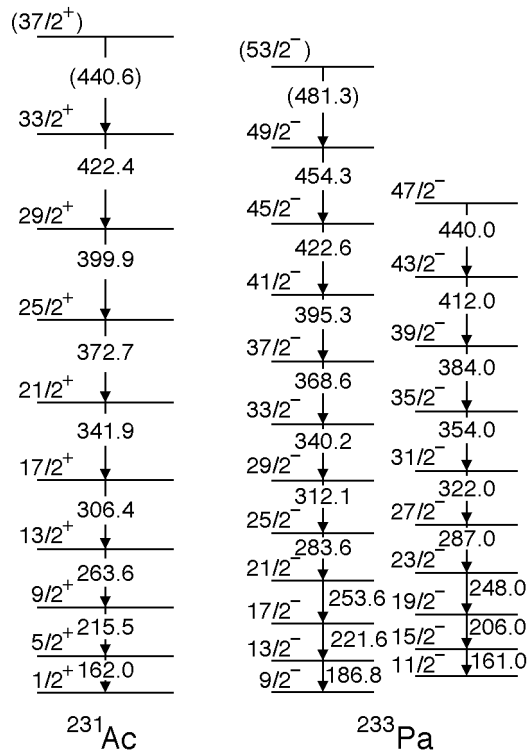


Fig. I-35. Preliminary level schemes for  $^{233}\text{Pa}$  and  $^{231}\text{Ac}$  obtained with the  $^{209}\text{Bi} + ^{232}\text{Th}$  reaction.

### b.27. Octupole Correlations in Pu Isotopes Studied by Coulomb Excitation

(I. Wiedenhöver, R. V. F. Janssens, K. Abu-Saleem, I. Ahmad, M. Alcorta, H. Amro, M. P. Carpenter, J. P. Greene, G. Hackman, T. L. Khoo, T. Lauritsen, C. J. Lister, D. T. Nisius, P. Reiter, D. Seweryniak, J. Uusitalo, S. Siem,\* J. Cizewski,† A. O. Macchiavelli,‡ P. Chowdhury,§ E. H. Seabury,§ D. Cline,¶ and C. Y. Wu¶)

We performed a series of measurements with Gammasphere at ATLAS, using the technique of "Unsafe Coulomb Excitation" to investigate the nuclear structure of Actinide nuclei around Plutonium. These experiments rely on a combination of facilities, which at this moment is only available at Argonne: The access to radiochemical and target production facilities to handle targets of Actinide Isotopes, the ATLAS accelerator, which provides beams of the heaviest ions at the required energy and intensity and Gammasphere, the world's most powerful gamma detector array.

In our experiments, we bombarded targets of the isotopes  $^{240}\text{Pu}$  and  $^{244}\text{Pu}$  with a  $^{208}\text{Pb}$  beam and  $^{239}\text{Pu}$ , and  $^{242}\text{Pu}$  targets with a  $^{207}\text{Pb}$  beam at energies

above the Coulomb barrier. The data includes Coulomb excitation of the target isotope as well as one- and two neutron transfer channels, which were central to establish detailed spectroscopic data for nuclei which are too short-lived to be used as target material, like  $^{238}\text{Pu}$  ( $T_{1/2} = 8$  y),  $^{241}\text{Pu}$  ( $T_{1/2} = 14$  y) and  $^{243}\text{Pu}$  ( $T_{1/2} = 5$  h).

A common feature for the excited states known in many actinide nuclei is the presence of a positive parity rotational band and a negative parity excited band, which is interpreted to be based on an octupole surface vibration. The combined data of our experiments yielded a detailed picture of nuclear structure for the odd and even mass nuclei between  $^{238}\text{Pu}$  and  $^{244}\text{Pu}$

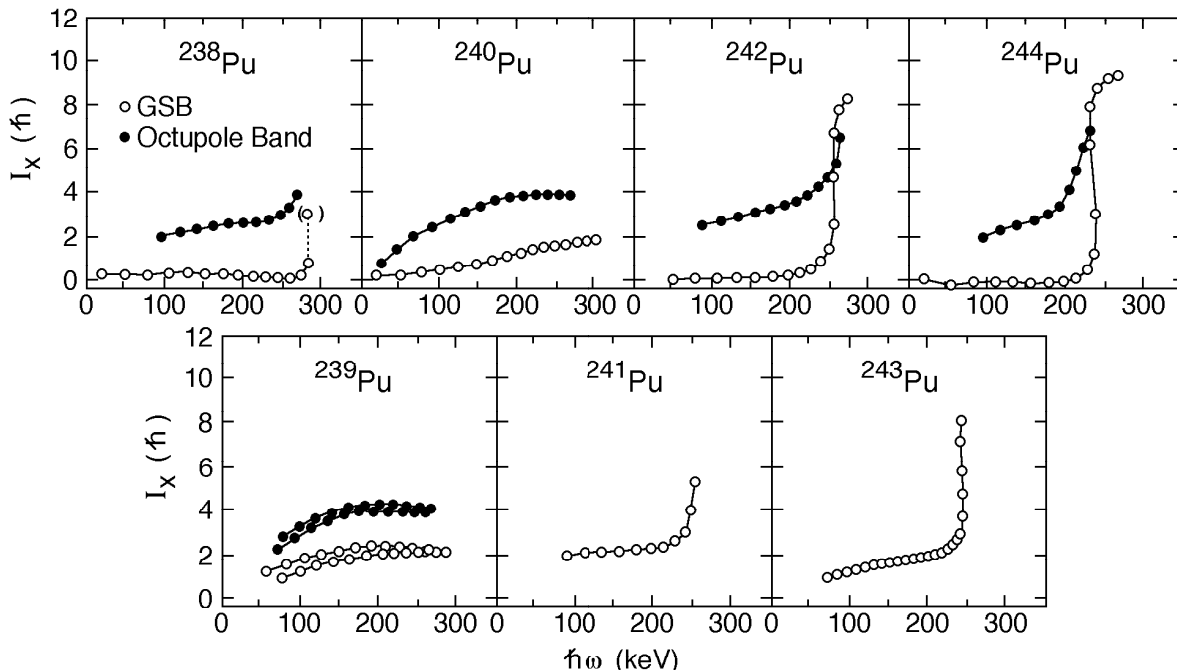


Fig. I-36. Aligned spins  $i_x$  of the yrast and octupole rotational bands in the Pu isotopes. In all cases the same reference is subtracted, with the Harris Parameters  $J_0 = 65 \hbar^2 \text{ MeV}^{-1}$  and  $J_1 = 369 \hbar^2 \text{ MeV}^{-3}$ .

and allowed us to investigate the properties of these two bands systematically. The results discussed below show an unexpected contrasting behavior between  $^{239}\text{Pu}$  and  $^{240}\text{Pu}$  and the other isotopes<sup>1</sup>. Figure I-36 shows the aligned angular momentum as a function of rotational frequency. For  $^{242}\text{Pu}$  and  $^{244}\text{Pu}$ , the curves show a behavior typical for the alignment of a pair of  $i_{13/2}$  protons due to the Coriolis force. The odd mass nuclei  $^{243}\text{Pu}$  and  $^{241}\text{Pu}$  show the same behavior. With the same certainty that this phenomenon was established in  $^{242}\text{Pu}$  and  $^{244}\text{Pu}$ , it was established to be missing in  $^{240}\text{Pu}$ . The absence or delay of such quasiparticle alignment was theoretically predicted in the presence of octupole deformation<sup>2</sup>.

Figure I-37 compares the relative energy position of the negative parity and positive parity bands for the even mass nuclei as a function of angular momentum. For high angular momenta, the negative parity band in  $^{240}\text{Pu}$  comes down to the energy of the ground state band. At the same time we could observe the two negative parity bands of  $^{239}\text{Pu}$  approach their respective positive parity partner, forming so-called "parity-doublers" at high angular momenta, which again is an expected property of octupole-deformed nuclei.

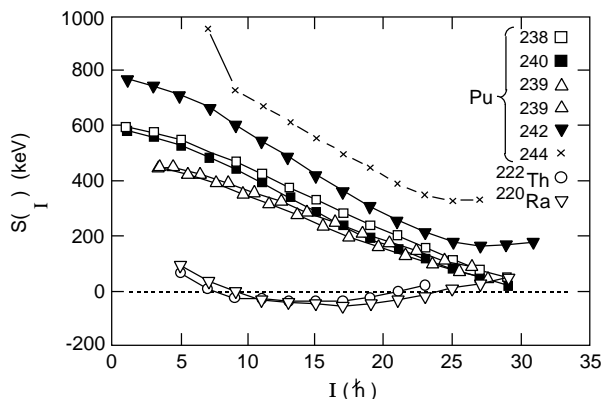


Fig. I-37 Comparison of the energy staggering  $S(I)$  as a function of spin  $I$  in the Pu isotopes and in  $^{220}\text{Ra}$  and  $^{222}\text{Th}$ , two of the best examples of octupole deformed nuclei.

Figure I-38 displays the electric dipole (E1)-transition matrix elements observed in the decay of the negative parity band to the positive parity partner. The decay of the  $^{240}\text{Pu}$  negative-parity band exhibits the largest transition dipole moments among the isotopes under investigation. This fact also points to the presence of strong octupole correlations or octupole deformation, which are expected to enhance E1-decays.

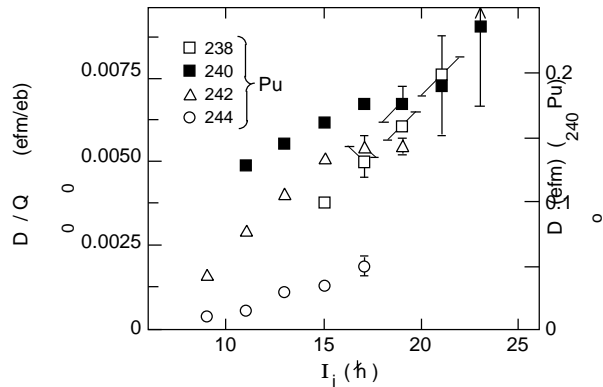


Fig. I-38. Ratio of transition dipole and quadrupole moments extracted from the E1 and E2 branchings E1:  $\Gamma_i (I_i-1)^+$ /E2:  $\Gamma_i (I_i-2)^-$  as a function of the spin  $I_i$ . The values of the transition dipole moment  $D_0$  given on the right hand side are for  $^{240}\text{Pu}$  only, where they have been calculated assuming rotational E2-matrix elements with the  $Q_0$  moment of the ground state band.

These three observables suggest that for the cases of  $^{240}\text{Pu}$  and  $^{239}\text{Pu}$  a transition has occurred from a situation, where octupole vibrations coexist with rotational behavior into a situation, where the ground state and octupole vibrational bands merge into one excitation associated with an octupole deformed shape. Although this transformation had been postulated for other nuclei, such as the neutron-deficient Th and Ra isotopes, this is the first observed case in nuclei with a strong quadrupole deformation. Furthermore, the octupole collectivity develops in a sharp transition along the Pu-isotope chain, which is a strong indication for a microscopic origin of this phenomenon. This observation at the same time poses a challenge for detailed microscopic calculations.

\*Argonne National Laboratory and University of Oslo, Norway, †Argonne National Laboratory and Rutgers University, ‡Lawrence Berkeley National Laboratory, §University of Massachusetts, ¶University of Rochester

<sup>1</sup>I. Wiedenhöver *et al.*, Phys. Rev. Lett. **83**, 2143 (1999).

<sup>2</sup>S. Frauendorf and V. Pashkevitch, Phys. Lett. **B141**, 23 (1984).

**b.28. Proton Transfer Reactions on  $^{237}\text{Np}$ ,  $^{241}\text{Am}$  and  $^{248}\text{Cm}$**  (R. V. F. Janssens, Ahmad, D. L. Bowers, J. Caggiano, M. P. Carpenter, J. P. Greene, A. Heinz, T. L. Khoo, F. G. Kondev, T. Lauritsen, C. J. Lister, D. Seweryniak, I. Wiedenhoever, K. Abu Saleem,\* G. Hackman,† P. Chowdhury,‡ D. Cline,§ M. Devlin,¶ N. Fotiades,¶ A. O. Macchiavelli,| E. H. Seabury,¶ and C. Wu§)

Following the successful study of proton transfer reactions with  $^{209}\text{Bi}$  beams on  $^{232}\text{Th}$  at energies ~ 20% above the Coulomb barrier, the resolving power of Gammasphere was used to study similar reactions on  $^{237}\text{Np}$ ,  $^{241}\text{Am}$  and  $^{248}\text{Cm}$ . The main goals of the measurements can be summarized as follows:

1. Study the behavior with spin and frequency of the proton excitations in  $^{237}\text{Np}$  and  $^{241}\text{Am}$  in relation to the alignment in the Pu and Cm even-even isotopes (possible blocking of proton alignment).
2. Study the octupole excitations in  $^{237}\text{Np}$  and  $^{241}\text{Am}$  and see whether they follow the pattern found for the same excitation in  $^{239}\text{Pu}$  (i.e. a transition from octupole vibration to octupole rotation) or whether they exhibit a

particle alignment instead (as in the heavier Pu isotopes).

3. Study the yrast and the lowest octupole band in  $^{242}\text{Cm}$  and determine whether the band sequences mirror those of the isotone  $^{240}\text{Pu}$  indicating similar octupole strength or whether they are similar to the patterns seen in the heavier Pu isotopes and in the isotone  $^{238}\text{U}$  (upbending or backbending in both the yrast and octupole bands).
4. Delineate for the first time excitations to high spin in  $^{249}\text{Bk}$  and  $^{250}\text{Cf}$  as well as in all other transfer channels populated in the reaction.

The 6 days experiment was performed with a 1450 MeV  $^{209}\text{Bi}$  beam. For each target a large statistical data set was collected. The data is under analysis.

---

\*Argonne National Laboratory and Illinois Institute of Technology, †University of Kansas, ‡University of Massachusetts-Lowell, §University of Rochester, ¶Los Alamos National Laboratory, |Lawrence Berkeley National Laboratory

- b.29. Spectroscopy of the Transfermium Nucleus  $^{252}\text{No}$**  (T. L. Khoo, C. J. Lister, R.-D. Herzberg,\* P. A. Butler,\* N. Amzal,\* A. J. C. Chewter,\* N. Hammond,\* G. D. Jones,\* R. D. Page,\* C. Scholey,\* O. Stezowski,\* M. Leino,† R. Julin,† J. F. C. Cocks,† O. Dorvaux,† P. T. Greenlees,† K. Helariutta,† P. M. Jones,† S. Juutinen,† H. Kankaanpaa,† H. Kettunen,† P. Kuusiniemi,† M. Muikku,† P. Nieminen,† P. Rakhila,† W. H. Trzaska,† F. Heberger,‡ J. Gerl,‡ Ch. Schlegel,‡ H. J. Wollersheim,‡ W. Korten,§ F. Becker,§ Y. Le Coz,§ K. Hauschild,§ M. Houry,§ R. Lucas,§ Ch. Theisen,§ P. Reiter,¶ and K. Eskola||)

The motivation for studying nobelium isotopes is given in Sec. b.34. This section reports on results from an experiment on  $^{252}\text{No}$ , conducted with JUROSPHERE II and RITU at Jyväskylä, with R. Herzberg as spokesperson. The behavior at high-spin of the moment of inertia of the ground state band and the comparison with that of  $^{252}\text{No}$  will reveal indirect information on the single-particle orbitals near the Fermi level, especially on the high-j ones, which align and increase the moment of inertia. In particular, the influence of the  $j_{15/2}$  orbitals is expected to lead to a

larger increase in the moment of inertia in  $^{252}\text{No}$  than in  $^{254}\text{No}$ .

From the experiment, the ground state band of  $^{252}\text{No}$  has been tentatively identified up to spin 20. The moment of inertia of  $^{252}\text{No}$  starts out lower than that of  $^{254}\text{No}$  at low frequency, but becomes larger at  $\omega \sim 0.14$  MeV, as it increases more rapidly. These results support the expectations based on the cranked shell model, using single-particle levels given by a Wood-Saxon potential with the measured deformation<sup>1</sup>.

\*University of Liverpool, United Kingdom, †University of Jyväskylä, Finland, ‡GSI Darmstadt, Germany, §DAPNIA/SPhN CEA-Saclay, France, ¶Ludwig Maximilians Universität München, Germany, ||University of Helsinki, Finland

<sup>1</sup>P. Reiter *et al*, Phys. Rev. Lett. **82**, 509 (1999).

- b.30. Entry Distribution of  $^{220}\text{Th}$  The Measurement of Fission Barriers at High Angular Momentum** (T. L. Khoo, I. Ahmad, M. P. Carpenter, C. N. Davids, J. P. Greene, A. Heinz, W. F. Henning, R. V. F. Janssens, F. G. Kondev, T. Lauritsen, C. J. Lister, D. Seweryniak, A. A. Sonzogni, J. Uusitalo, I. Wiedenhöver, P. Reiter,\* P. Bhattacharyya,† J. A. Cizewski,‡ G. D. Jones,§ R. Julin,¶ and S. Siem||)

Today, more than 60 years after the discovery of nuclear fission, the number of nuclei, whose fission barriers have been experimentally determined, is still very limited. In the past, fission induced by neutrons or charged particles allowed an accurate measurement of fission barriers of fissile nuclei in the vicinity of stable or long-lived targets. Fission induced by photons and electrons provided similar information.

they are essential for understanding the production mechanisms of superheavy elements.

We have introduced a new method, which uses the entry distribution for an evaporation residue, to set constraints on the fission barrier of the shell stabilized nucleus  $^{254}\text{No}$  - see Ref. 1.

Far off stability different methods have been applied. Pioneering work has been done using beta-delayed fission or electromagnetic interaction of relativistic secondary beams with Pb targets. These methods are limited as well: in the former case only nuclei which show beta-delayed fission are accessible. In the latter case, an intense primary beam is needed, which excludes elements heavier than Pu. The fission barriers of the heaviest elements are particularly interesting, as

Here, we report on the measurement of the entry distribution of  $^{220}\text{Th}$ . A  $^{48}\text{Ca}$  beam at 206 MeV was used to produce  $^{220}\text{Th}$  in a fusion reaction with a 810  $\mu\text{g}/\text{cm}^2$  target of  $^{176}\text{Yb}$ . The energy was chosen in order to maximize the production cross section, which is expected to be about 1 mb (Ref. 2). As the fission barrier of  $^{220}\text{Th}$  has been determined before using electromagnetic interaction of relativistic secondary beams<sup>3</sup>, it provides a calibration of the entry distribution method. In addition, the method provides the first direct measurement of the spin dependence of

the fission barrier. The fission barrier of  $^{220}\text{Th}$  should be dominated by its liquid drop term; therefore a strong spin dependence is expected. This is in contrast to  $^{254}\text{No}$ , where the fission barrier arises predominantly from the shell energy. Our entry distributions<sup>1</sup> in  $^{254}\text{No}$  suggest that the shell-correction energy and, hence, the fission barrier is robust against rotation.

The preliminary entry distribution of  $^{220}\text{Th}$  is shown in Fig. I-39. The distribution does not extend beyond the

neutron separation energy  $S_n$  - as expected - and is mainly confined within the locus of the saddle-point energy  $E_{\text{saddle}}$ . The data suggest that the fission barrier, at e.g. spin 20, is larger than 6.5 MeV, which is somewhat higher than the predicted value of 5.7 MeV. This compares to the value  $B_f = 6.8$  obtained by Grewe *et al.*<sup>3</sup> at spin 0.

Further analysis, especially of a data set at higher excitation energies, is in progress.

\*LMU University of Munich, Germany, †Purdue University, ‡Argonne National Laboratory and Rutgers University, §University of Liverpool, United Kingdom, ¶University of Jyväskylä, Finland, ||Argonne National Laboratory and University of Oslo, Norway

<sup>1</sup>P. Reiter *et al.*, see Sec. b.34; Phys. Rev. Lett., in press; Phys. Rev. Lett. **82**, 509 (1999).

<sup>2</sup>C. C. Sahm *et al.*, Nucl. Phys. **A441**, 316 (1985).

<sup>3</sup>A. Grewe *et al.*, Nucl. Phys. **A614**, 400 (1997).

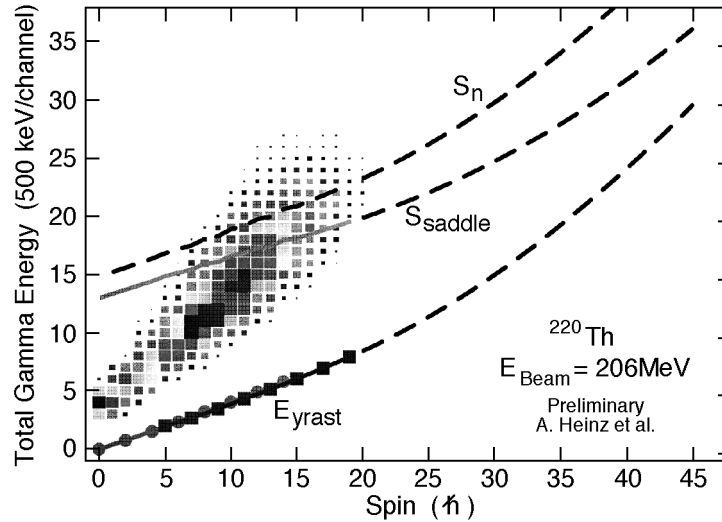


Fig. I-39. Preliminary entry distribution of  $^{220}\text{Th}$ . The yrast line, the neutron-separation energy  $S_n$  and the saddle-point energy  $E_{\text{saddle}}$  are shown. The saddle-point energy is defined as  $E_{\text{saddle}}(I) = E_{\text{yrast}}(I) + B_f(I)$ , with  $B_f(I)$  being the fission barrier at a given angular momentum  $I$ .  $B_f(I)$  is calculated as the sum of a liquid drop and ground-state shell correction terms. The dashed lines are extrapolations. The neutron separation energy is calculated according to  $S_n(I) = S_n(I=0) + E_{\text{yrast}}(I)$ .

**b.31. Correlated Spins of Complementary Fragment Pairs in the Spontaneous Fission of  $^{252}\text{Cf}$**  (I. Ahmad, J. P. Greene, A. G. Smith,\* G. S. Simpson,\* J. Billowes,\* P. J. Dagnall,\* J. L. Durell,\* S. J. Freeman,\* M. Leddy,\* W. R. Phillips,\* A. A. Roach,\* J. F. Smith,\* A. Jungclaus,† K. P. Lieb,† C. Teich,† B. J. P. Gall,‡ F. Hoellinger,‡ N. Schulz,‡ and A. Algora§)

Investigations of the properties of fission-fragment angular momentum provide one of the few means open to the experimentalist to explore the behavior of the fissioning system near the point of scission, providing a particularly crucial test in the case of spontaneous fission where the initial angular momentum of the system is well defined.

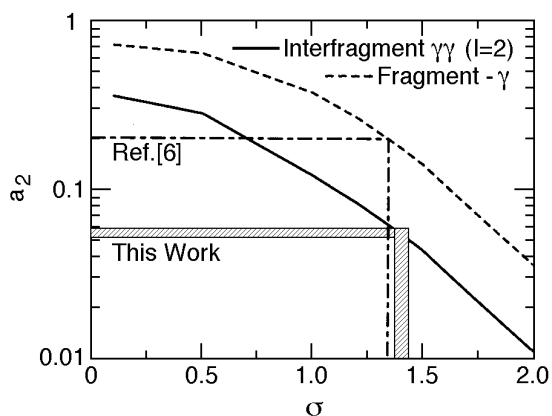


Fig. I-40. Results of calculations of  $m$ -substate smearing and its effect on the  $a_2$  coefficient for fragment- angular distributions, as well as correlations between the  $2 \rightarrow 0$  decays of complementary fragment pairs.

A  $120 \mu\text{Ci } ^{252}\text{Cf}$  source, sandwiched between two  $20 \text{ mg cm}^{-2}$  Gd foils, was used as a source of neutron-rich fission fragments, whose  $\gamma$ -ray decays were detected in the Euroball array of germanium detectors. In this experiment measurements were made of angular correlations between  $\gamma$  rays emitted from one fragment with  $\gamma$  rays from the complementary fragment, for decays from low-lying excited states. For a range of complementary fragment pairs, the inter-fragment correlation was measured between the  $2_1 \rightarrow 0_1$  -ray in

the heavy fragment and the  $2_1 \rightarrow 0_1$  -ray in the light fragment. Measurements were also made of the inter-fragment angular correlations between  $4_1 \rightarrow 2_1$  rays. For complementary even-even fragments the weighted mean inter-fragment anisotropy, for  $2 \rightarrow 0, 2 \rightarrow 0$  coincidences was found to be  $A = 0.101(7)$  with weighted mean values  $a_2 = 0.057(4)$  and  $a_4 = 0.021(5)$ . The corresponding result for  $4 \rightarrow 2, 4 \rightarrow 2$  inter-fragment coincidences was  $A = 0.05(1)$  with weighted mean values of  $a_2 = 0.035(5)$  and  $a_4 = -0.003(8)$ . Data from a previous experiment using a  $^{248}\text{Cm}$  fission source<sup>1</sup> was re-analyzed with a method analogous to that used for  $^{252}\text{Cf}$ . The weighted mean inter-fragment  $\gamma$ -ray anisotropy for  $2 \rightarrow 0, 2 \rightarrow 0$  coincidences was found to be  $A = 0.016(4)$  with weighted mean coefficients  $a_2 = 0.014(2)$  and  $a_4 = -0.009(3)$ . We adopt a similar Gaussian smearing technique to that used by Yamazaki<sup>2</sup> for parameterizing the degree of alignment in heavy-ion fusion-evaporation reactions. The  $z$ -direction is defined by the  $\gamma$  ray from one fragment and full alignment corresponds to the  $m$ -substate populations in the two fragments being equal. Figure I-40 shows the effect of varying  $\sigma$  on the  $a_2$  coefficient for inter-fragment correlations, assuming two quadrupole  $2 \rightarrow 0$  transitions, as well as for fragment-distributions with a quadrupole  $2 \rightarrow 0$  decay. The measured value of  $a_2 = 0.057(5)$  for the inter-fragment correlations in  $^{252}\text{Cf}$  indicates a statistical width  $\sigma = 1.40(5)$ . The magnitude of the corresponding theoretical  $a_4 (= -0.01)$  is very much attenuated at this value of  $\sigma$ . The fragment- distributions of Wilhelmy et al.<sup>3</sup> for  $2 \rightarrow 0$  decays in  $^{100,102}\text{Zr}$ ,  $^{104,106}\text{Mo}$ ,  $^{110}\text{Ru}$ ,  $^{144}\text{Ba}$  and  $^{148}\text{Ce}$ , produced in the spontaneous fission of  $^{252}\text{Cf}$ , have a mean value of  $a_2 = 0.20(4)$ . As seen in Fig. I-40, this translates into a statistical substate smearing with  $\sigma = 1.35(5)$ . The similarity in the smearing widths for inter-fragment

\*University of Manchester, United Kingdom, †University of Göttingen, Germany, ‡IREs and University of Louis Pasteur, Strasbourg, France, §Laboratori Nazionali Legnaro, Italy

<sup>1</sup>M. A. Jones *et al.*, Nucl. Phys. **A605**, 133 (1996).

<sup>2</sup>T. Yamazaki, Nucl. Data. **3**, 1 (1967).

<sup>3</sup>J. B. Wilhelmy *et al.*, Phys. Rev. C **5**, 2041 (1972).

<sup>4</sup>A. G. Smith *et al.*, Phys. Rev. C **60**, 064611 (1999).

correlations and fragment- distributions in  $^{252}\text{Cf}$  fission is somewhat surprising given that the correlations suffer from substate smearing from two independent statistical processes, the deexcitation to the  $2^+$  states in two fragments, whereas the fragment-distributions suffer attenuation due to the statistical decay in one fragment only. This suggests that there is

an additional statistical process which contributes to the substate smearing in fragment- distributions, but does not affect the inter-fragment correlations. One possible explanation is that the fragment spins are not mutually parallel, but are tilted out of the plane perpendicular to the fission axis. The results of this investigation were published<sup>4</sup>.

### b. 32. Relative Cross Sections for Production of $^{253,254}\text{No}$ and Their Detection Efficiencies

(T. L. Khoo, I. Ahmad, M. P. Carpenter, C. N. Davids, A. Heinz, W. F. Henning, R. V. F. Janssens, F. Kondev, T. Lauritsen, C. J. Lister, D. Seweryniak, S. Siem, A. A. Sonzogni, I. Wiedenhöver, P. Reiter,\* N. Amzal,† P. A. Butler,‡ J. Chewter,‡ J. A. Cizewski,‡ P. T. Greenlees,† K. Helariuta,§ R. D. Herzberg,† G. Jones,† R. Julin,§ H. Kankaanpää,§ W. Korten,¶ M. Leino,§ J. Uusitalo,§ K. Vetter,|| H. Kettunen,§ P. Kuusiniemi,§ and M. Muikku§)

In order to study the nuclear structure of the shell-stabilized nuclei, it is necessary to first know the production cross sections. The relative cross sections for the  $^{207,208}\text{Pb}(^{48}\text{Ca},2n)^{253,254}\text{No}$  reactions have been measured with the gas-filled separator RITU at Jyväskylä. By taking a cross section<sup>1</sup> of  $2\ \mu\text{b}$  for  $^{254}\text{No}$ , the cross section of  $^{253}\text{No}$  was determined to be  $0.46\ \mu\text{b}$ , with an uncertainty of  $\sim 30\%$ . During a subsequent experiment to investigate the structure of  $^{253}\text{No}$  with Gammasphere and the Fragment Mass Analyzer (FMA), it was unexpectedly found that the focal-plane detection rates of the two nobelium isotopes was about the same (within 30%). This implies that the FMA detection efficiency of the mass 254 isotope is about a quarter that of the mass 253 isotope. The probable explanation is that there is an isomer, with half life  $0.1\text{-}3\ \mu\text{s}$ , in  $^{254}\text{No}$ . The decays within the FMA, with a flight time of  $1.5\ \mu\text{s}$ , would change the charge state, resulting in trajectories that do not land on the focal-plane detectors. On the other hand, rapid re-equilibration of the charge state in the gas of RITU would keep the trajectories of the evaporation residues close to normal, so that there is no loss of detection efficiency. Confirmation of this hypothesis would

come from detection of an isomer in  $^{254}\text{No}$ , with a lifetime in the  $\mu\text{s}$  range, in a future experiment.

These results have implications in the search for superheavy elements, which are likely to have isomers, especially in spherical nuclei with doubly-closed shells. (There are many known isomers near  $^{208}\text{Pb}$ .) If the lifetimes are similar to the flight times through vacuum-based separators, such as the FMA and SHIP (at GSI), then the detection efficiencies of superheavy elements would be reduced. This may be a possible explanation for the different results on element 118: three events were detected in the gas-filled BGS separator at LBNL, whereas none were detected at SHIP with comparable integrated beam. Although this is only a speculation at this time, nevertheless one has to seriously take into account the role of isomers in the search for superheavy elements. Our investigations on the nobelium isotopes have emphasized that, to reach the ground state, an evaporation residue has to decay by gamma cascades from excited entry states of moderate spin. Isomers along the cascade have more deleterious consequences if the decay occurs within vacuum separators than in gas-filled separators.

\*Ludwig-Maximilians-Universität, Garching, Germany, †University of Liverpool, United Kingdom, ‡Rutgers University, §University of Jyväskylä, Finland, ¶DAPNIA/SPhN, CEA Saclay, France, ||Lawrence Berkeley National Laboratory

<sup>1</sup>M. Leino *et al.*, Eur. Phys. J **A6**, 63 (1999).

- b.33. Structure, Fission Barrier and Limits of Stability of  $^{253}\text{No}$**  (T. L. Khoo, I. Ahmad, M. P. Carpenter, C. N. Davids, A. Heinz, W. F. Henning, R. V. F. Janssens, F. Kondev, T. Lauritsen, C. J. Lister, D. Seweryniak, S. Siem, A. A. Sonzogni, I. Wiedenhöver, P. Reiter,\* N. Amzal,† P. A. Butler,† A. J. Chewter,† J. A. Cizewski,‡ P. T. Greenlees,† K. Helariuta,§ R. D. Herzberg,† G. Jones,† R. Julin,§ H. Kankaanpää,§ W. Korten,¶ M. Leino,§ J. Uusitalo,§ K. Vetter,|| H. Kettunen,§ P. Kuusiniemi,§ and M. Muikku§)

For the heaviest nuclei, including the superheavy nuclei, a large shell-correction energy provides additional binding, thereby creating a fission barrier where none (or a small one) would have existed. Knowledge of the single-particle energies of the heaviest nuclei is important for calculating the shell-correction energy. The most direct information on the single-particle energies comes from an odd nucleus,  $^{253}\text{No}$  in this case. The entry distribution gives information on the fission barrier – see Secs. b.30 and b.34. It is interesting to determine the mass dependence of the fission barrier around  $N = 152$  for two reasons. First, the barrier has been found to vary rapidly near  $N = 152$  for lighter nuclei. Second, barriers of a sequence of isotopes provide a good test of theory.

For these reasons, we have performed an experiment to study the levels of  $^{253}\text{No}$ , with the use of the  $^{207}\text{Pb}(^{48}\text{Ca},2n)$  reaction. In a first experiment with the gas-filled separator RITU at Jyväskylä, the production cross section of  $^{253}\text{No}$  was measured as  $\sim 0.5 \mu\text{b}$  (by comparing with the known cross section for the  $^{208}\text{Pb}(^{48}\text{Ca},2n)^{254}\text{No}$  reaction). This showed that a  $\gamma$ -ray experiment was feasible.

In a subsequent experiment at Argonne, the  $\gamma$  rays were detected with Gammasphere, in coincidence with the

FMA, as described in Sec. b.34. It is clear that in  $^{253}\text{No}$  the spectrum is dominated by the K X-rays and that the transitions connecting excited states are much weaker relative to the x-rays. (The integrated beam for the odd-nucleus experiment was about three times larger.) The explanation for the difference lies in a huge conversion electron branch for  $I = 1$  intraband transitions in the odd nucleus. Even with a small M1 branching ratio, there is an overwhelmingly large conversion electron yield. Analysis is in progress in an attempt to assign the observed transitions within rotational bands. However, it is likely that many of the observed gamma rays probably represent interband transitions (probably of E1 character, which have smaller conversion coefficients).

We have also measured the two-dimension distribution in detector multiplicity vs. the sum energy. A tail of high fold, with low sum energy, is observed, in  $^{253}\text{No}$ , which is absent in  $^{254}\text{No}$ . This tail is most likely from dipole transitions. There is nonetheless a significant contribution from stretched E2 transitions in both nuclei. This component suggests smaller sum energy, but a higher fold, in the odd nucleus. Although the analysis is preliminary at this stage, the lower sum energy already points towards a lower fission barrier in  $^{253}\text{No}$  than in  $^{254}\text{No}$ .

\*Ludwig-Maximilians-Universität, Garching, Germany, †University of Liverpool, United Kingdom, ‡Rutgers University, §University of Jyväskylä, Finland, ¶DAPNIA/SPhN, CEA Saclay, France, ||Lawrence Berkeley National Laboratory

**b.34. Entry Distribution, Fission Barrier, Formation Mechanism and Structure of  $^{254}\text{No}$**   
 (P. Reiter, T. L. Khoo, I. Ahmad, M. P. Carpenter, C. N. Davids, J. P. Greene, A. Heinz, W. F. Henning, R. V. F. Janssens, F. G. Kondev, T. Lauritsen, C. J. Lister, D. Seweryniak, A. Sonzogni, J. Uusitalo, I. Wiedenhöver, N. Amzal,\* P. Bhattacharyya,† P. A. Butler,\* J. Chewter,\* J. A. Cizewski,‡ K. Y. Ding,§ N. Fotiades,§ P. T. Greenlees,\* R.-D. Herzberg,\* G. D. Jones,\* W. Korten,¶ M. Leino,|| S. Siem,\*\* and K. A. Vetter††)

The heaviest nuclei, with  $Z > 100$ , are at the limit of Coulomb instability. They would be unstable against spontaneous fission but for a large shell-correction energy, which leads to additional binding and creates a sizeable fission barrier of up to 8 MeV. The existence of these very heavy elements is a striking manifestation of shell structure in nuclei, and arises from the identical mechanism responsible for the proposed stability of an “island” of superheavy elements around  $Z = 114$ ,  $N = 184$ . Recent reports<sup>1,2</sup> of the detection of elements 114 and 116, 118 provide support for the stability of superheavy elements. Shell-stabilized nuclei could be different from ordinary nuclei, where the binding is largely derived from the liquid-drop energy. However, there is little experimental information on the properties of shell-stabilized nuclei. Their high-spin behavior, e.g. the variation with spin of the moment of inertia and of the fission barrier, would provide information about the angular momentum dependence of the shell energy, which is not only interesting in its own right, but also provides a new test of theories that calculate the properties of superheavy elements. Since the heaviest nuclei are only weakly bound in the ground state, it is interesting to determine the limiting spin and excitation energy that they can sustain. The limits of stability in spin and excitation energy are governed by the fission barrier. Knowledge of the barrier is also essential for understanding the production mechanism of superheavy nuclei.

In lighter actinide nuclei the fission barrier parameters are most directly obtained in nucleon-transfer or neutron-capture reactions from the variation of the fission probability as a function of excitation energy  $E^*$ . Since no suitable target exists, this method is not applicable to the heaviest elements. We propose a new method that may be used to deduce the fission barrier  $B_f(I)$  and also its variation with spin  $I$ . The method is based on a measurement of the entry distribution, which represent the distribution of initial states from which gamma decay to the ground state start. Hence, the entry distribution reflect states where gamma emission successfully compete with fission and the distribution is generally located below the fission barrier.

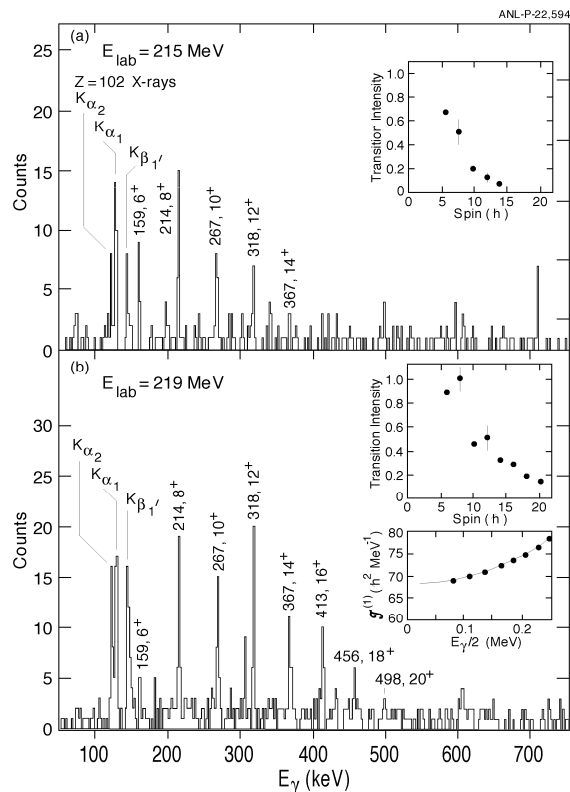


Fig. 1-42.  $^{254}\text{No}$  spectra at beam energies of (a) 215 MeV and (b) 219 MeV. The gsb transitions are labeled by their energies (in keV) and initial spins. Note the large increase in high-spin population at the higher beam energy, which is also seen in the insets that show relative intensities (with some typical statistical errors). A second inset in Fig. 1-42(b) shows the moment of inertia ( $I$ ) vs.  $E/2$ .

We have measured the entry distributions of  $^{254}\text{No}$ , which is an example of a shell-stabilized nucleus. The reaction  $^{208}\text{Pb}(^{48}\text{Ca}, 2n)^{254}\text{No}$  was used to populate states in  $^{254}\text{No}$ . Gammasphere was used to measure not only the  $\gamma$  rays with high resolution, but also the  $\gamma$ -ray multiplicity and sum energy. The  $\gamma$  rays from  $^{254}\text{No}$  nuclei were extracted from a background due to fission, which was  $> 10^4$  times more intense, by requiring coincidences with evaporation residues. The latter were unambiguously identified with the Argonne

Fragment Mass Analyzer (FMA). To minimize deterioration of the  $^{208}\text{Pb}$  targets ( $\sim 0.5 \text{ mg/cm}^2$ ), they were mounted on a rotating wheel and the beam was wobbled vertically  $\pm 2.5 \text{ mm}$  across the target with a magnetic steerer. Beams with energies of 215 MeV and 219 MeV and intensities of 9 pA to 12 pA were provided by ATLAS. The compound nucleus (CN) excitation energies (at mid target) were 19.3 MeV and 22.7 MeV, respectively. The spectra obtained at 215 MeV, which we have previously published<sup>3</sup>, and at 219 MeV are compared in Fig. I-42. Transitions from

higher-spin members of the ground state band (gsb) are clearly enhanced at the higher bombarding energy and the gsb could be extended up to spin  $20^+$  [Fig. I-42(b)]. The relative transition intensities, given in the insets, show that the population has saturated by spin 8 at the higher beam energy.

In order to determine the initial angular momentum and excitation energy of the  $^{254}\text{No}$  residues, we measured the number of detector modules that fired and the total energy emitted by radiation. Based on measured response functions, a two-dimensional Monte Carlo unfolding procedure transformed the two-dimensional distribution of detector multiplicity vs. sum energy into a distribution of multiplicity vs. excitation energy. (To correct for the effect of the trigger requirement of two Compton suppressed Ge events, the efficiency dependence on multiplicity was taken into account.) The initial spin of the evaporation residue is deduced from the multiplicity. For high-Z nuclei, the internal conversion coefficients can be very large for low-energy transitions and estimates for electron multiplicities are made from the measured properties of the gsb.

The entry distributions, which represent the starting point for decay and formation of  $^{254}\text{No}$ , are shown in Fig. I-43 for the two beam energies. The one-dimensional spin and excitation energy distributions are also given. It is evident that a small increase in beam energy leads to noticeably higher initial spins and excitation energies. The entry distribution at the lower beam energy reveals that it is the maximum allowable energy  $E^*_{\text{max}}$  after neutron emission that imposes a  $16 \hbar$  limit on the angular momentum and not the fission barrier. At the higher beam energy, states up to spin  $22 \hbar$  and  $E^* = 8.5 \text{ MeV}$  (up to 6 MeV above the yrast line) are populated in the entry distribution, showing that the nucleus clearly can survive against fission up to these limits. At the higher beam energy, the entry distribution no longer extends to  $E^*_{\text{max}}$ , perhaps an indication of fission competition.

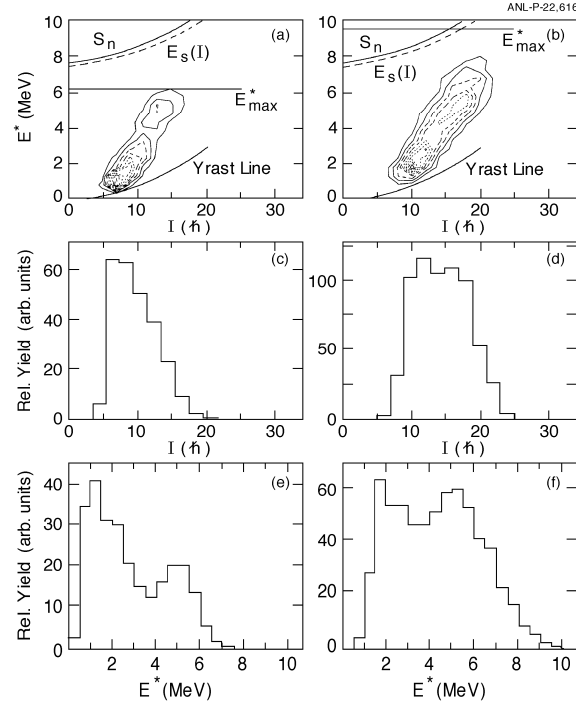


Fig. I-43. Contour plots (a,b) of the entry distributions in spin and excitation energy and their projections at  $E_{\text{Lab}} = 215$  (left panels) and 219 (right panels) MeV. The measured yrast line, the neutron-separation energy  $S_n$ , a theoretical saddle-point energy  $E_s(I)$  and the maximum allowable energy,  $E^*_{\text{max}} = E_{\text{CN}} - S_{n1} - S_{n2}$ , in  $^{254}\text{No}$  are indicated. The distributions in spin (c,d) and excitation energy (e,f) are also shown.

Gamma decay to the ground state originates from the entry distribution, implying successful competition over fission. The highest-energy point of the entry distribution for each spin lies below the saddle energy,  $E_s(I) = E_{\text{yrast}}(I) + B_f(I)$ , (or within 0.5 MeV), so that a lower bound on  $B_f(I)$  can be obtained. Only a lower bound on  $B_f$  can be deduced since the decreasing population with increasing excitation energy could, in principle, also be due to a reduced cross section after neutron emission. Energy distributions for individual spin bins, projected from the entry distributions in Fig. I-43(a,b), show that the half-maximum points correspond to 5 MeV above the yrast line for  $I = 12$ . This suggests that, even at high spin,  $B_f > 5 \text{ MeV}$ , a surprisingly large value for a nucleus as fissile as  $^{254}\text{No}$ .

There are no calculations of the shell-correction energy at higher spin, but if it were to remain constant with spin, the saddle-point energy,  $E_s(I)$ , would lie along the dashed line in Fig. I-43. The slight decrease from the

solid line denoting the neutron separation energy is due to the diminution of the liquid-drop term.

Our data provide new information important for understanding the synthesis of superheavy nuclei. Previously, the only constraints on theory have come from excitation function measurements of ground-state cross sections. The present results reveal that high partial waves contribute to the formation of evaporation residues, as predicted by Smolanczuk<sup>4</sup>. The fission barrier governs the survival of the compound nucleus, as it evaporates neutrons and  $\gamma$  rays in competition with fission decay. Fusion-evaporation calculations suggest that a barrier of 5 MeV would lead to a much larger cross section for production of <sup>254</sup>No than is observed<sup>5</sup>. This suggests either that there is a hindrance in the formation of the compound nucleus or that the fission barrier damps rapidly with excitation energy.

An unexpected feature of our entry distribution is the sharp tilt angle with respect to the yrast line. This is due, at least in part, to the small excitation energy of the low-spin entry states, which appears to be a distinct component [see Fig. I-43 (a,b,e,f)]. This feature cannot be easily explained by a simple statistical model. At low excitation energy, the level density is small, so that

states near the yrast line should have only small population. The deviation of the entry distribution from the line representing  $E^*_{\max}$  gives the energy removed by the 2 neutrons. Hence, evaporation residues with low partial waves appear to be associated with unusually energetic neutrons. On the other hand, at higher spin ( $I \approx 14$ ) the high excitation energy above the yrast line is more normal. Hence, there is a hint of at least two mechanisms in the formation of superheavy nuclei: a normal statistical one responsible for high-spin formation and another one with emission of higher energy (perhaps pre-equilibrium) neutrons, which is important at lower spins.

In summary, we have measured the entry distribution for a shell-stabilized nucleus. The limiting angular momentum and excitation energy are deduced for excited states in <sup>254</sup>No after the <sup>208</sup>Pb(<sup>48</sup>Ca,2n) reaction. The data provide direct information on the fission barrier and on the shell-correction energy, based on a novel experimental technique to determine a lower bound of the barrier height. In the synthesis of very heavy nuclei, the entry distributions suggest that high partial waves contribute and that there may be more than one reaction mechanism. A paper on this work has been submitted to Physical Review Letters.

\*University of Liverpool, United Kingdom, †Purdue University, ‡Argonne National Laboratory and Rutgers University, §Rutgers University, ¶DAPNIA/SPhN, CEA Saclay, France, || Ludwig-Maximilians-Universität, Garching, Germany, \*\*Argonne National Laboratory and University of Oslo, Norway, ††Lawrence Berkeley National Laboratory

<sup>1</sup>Yu. Ts. Oganessian *et al.*, Nature **400**, 242 (1999); Phys. Rev. Lett. **83**, 3154 (1999).

<sup>2</sup>V. Ninov *et al.*, Phys. Rev. Lett. **83**, 1104 (1999).

<sup>3</sup>P. Reiter *et al.*, Phys. Rev. Lett. **82**, 509 (1999).

<sup>4</sup>R. Smolanczuk, Phys. Rev. C **59**, 2634 (1999).

<sup>5</sup>H. W. Gäggeler *et al.*, Nucl. Phys. **A502**, 561c (1989).

**b.35. Jyväskylä Experiment on Excited States in  $^{254}\text{No}$**  (T. L. Khoo, M. Leino,\*  
 F. P. Hessberger,† R.-D. Herzberg,‡ Y. Le Coz,§ F. Becker,§ P.A. Butler,‡  
 J. Chewter,‡ J. F. C. Cocks,\* O. Dorvaux,\* K. Eskola,¶ J. Gerl,† P. T. Greenlees,‡  
 K. Helariutta,\* M. Houry,§ G. D. Jones,‡ P. M. Jones,\* R. Julin,\* S. Juutinen,\*  
 H. Kankaanpää,\* H. Kettunen,\* W. Korten,§ P. Kuusiniemi,\* R. Lucas,§ M. Muikku,\*  
 P. Nieminen,\* R. D. Page,‡ P. Rahkila,\* P. Reiter,|| A. Savelius,\* Ch. Schlegel,†  
 Ch. Theisen,§ W. H. Trzaska,\* and H.-J. Wollersheim†)

The nucleus  $^{254}\text{No}$  is one of the heaviest for which there is a possibility of investigating the excited states. The motivation for studying it has already been discussed above (see Sec. b.34). An experiment was conducted at Jyväskylä, which employed the SARI detector array together with the gas-filled recoil separator RITU to study the structure of  $^{254}\text{No}$ . The production reaction was  $^{48}\text{Ca} + ^{208}\text{Pb}$ . SARI consisted of four unshielded, segmented clover detectors placed at 50 degrees relative to the beam direction. Stationary  $^{208}\text{Pb}$  targets of 250-700  $\mu\text{g}/\text{cm}^2$  thickness were used. The beam current was 10 pA. An excitation function measurement found the maximum cross section of  $\sim 2$   $\mu\text{b}$  at a beam energy of 216 MeV (two-thirds into the

target), corresponding to 21 MeV excitation in the compound system. The method of recoil decay tagging (RDT) was used to identify in-beam gamma rays observed in the SARI detectors, on the basis of the 8.09 MeV alpha particles emitted by  $^{254}\text{No}$ .

The same transitions are observed in the RDT spectrum but with lower intensity due to the loss of escaping alpha particles. Ground state band transitions are observed up to 414 keV. The results confirm the transitions observed in the Argonne experiment and extend the ground band by one transition ( $16^+ - 14^+$ ).

This work has been published in Euro. Phys. J.

\*University of Jyväskylä, Finland, †GSI, Darmstadt, Germany, ‡University Liverpool, United Kingdom, §DAPNIA/SPhN CEA-Saclay, France, ¶University of Helsinki, Finland, ||Ludwig-Maximilians University, Munich, Germany

**b.36. Spectroscopic Studies Beyond N = 152 Neutron Gap: Decay of  $^{255}\text{Md}$  and  $^{256}\text{Md}$**   
 (I. Ahmad, R. R. Chasman, and P. R. Fields\*)

Energies of single-particle states in the heaviest nuclei accessible are needed to understand the structure of superheavy elements. In the early seventies we produced Md isotopes by the irradiation of  $^{253}\text{Es}$  with 35-45 MeV alpha particles from the Argonne 152 cm cyclotron. The recoiling Md atoms were stopped in He gas and were removed by a gas jet system. Alpha, gamma and alpha-gamma coincidence spectra of purified Md isotopes were measured by Si and Ge detectors. Gamma rays were assigned to  $^{255}\text{Md}$  and

$^{256}\text{Md}$  isotopes on the basis of their measured half-lives. The  $^{256}\text{Md}$  gamma rays could not be placed in a level scheme because the  $2^+ - 0^+$  transition energy in  $^{256}\text{Fm}$  ground state band was not known. The publication of the levels in  $^{256}\text{Fm}$  by Hall et al.<sup>1</sup> provided us the necessary information to interpret our data. In the case of  $^{255}\text{Md}$ , two gamma rays of energy 453.1 and 405.5 keV were observed in coincidence with  $^{255}\text{Md}$  alpha particles.

<sup>1</sup>H. L. Hall *et al.*, Phys. Rev. C **39**, 1866 (1989).

<sup>2</sup>I. Ahmad *et al.*, Phys. Rev. C **17**, 2163 (1978).

<sup>3</sup>I. Ahmad *et al.*, Phys. Rev. C **61**, 044301 (2000).

\*deceased

The same transitions were also seen in the electron capture decay of  $^{251}\text{Fm}$  and were interpreted as transitions deexciting the  $7/2^-$ -[514] single particle state at 460.4 keV. Since the 460.4 keV level in  $^{251}\text{Es}$  is populated by the favored alpha decay, the ground state of  $^{255}\text{Md}$  is established as the  $7/2^-$ -[514]. This is the only nucleus in which a definite identification of the  $7/2^-$ -[514] orbital has been made.

The  $^{256}\text{Md}$  nucleus is found to populate low spin states in  $^{256}\text{Fm}$ . The  $2^+$  vibrational band previously observed by Hall et al.<sup>1</sup> has been identified in the  $^{256}\text{Md}$  decay. In addition, four other levels have been identified which are given spin-parity assignments of  $1^+$ ,  $2^+$ ,  $1^-$ ,  $2^-$ . The level scheme of  $^{256}\text{Fm}$  is shown in Fig. I-45. These levels are interpreted as the  $nn\{7/2^+[613;9/2^+[615]]1^+$  and  $pp\{7/2^+[633];7/2^-[514]\}0^-$  bands. The results of this investigation were published.<sup>3</sup>

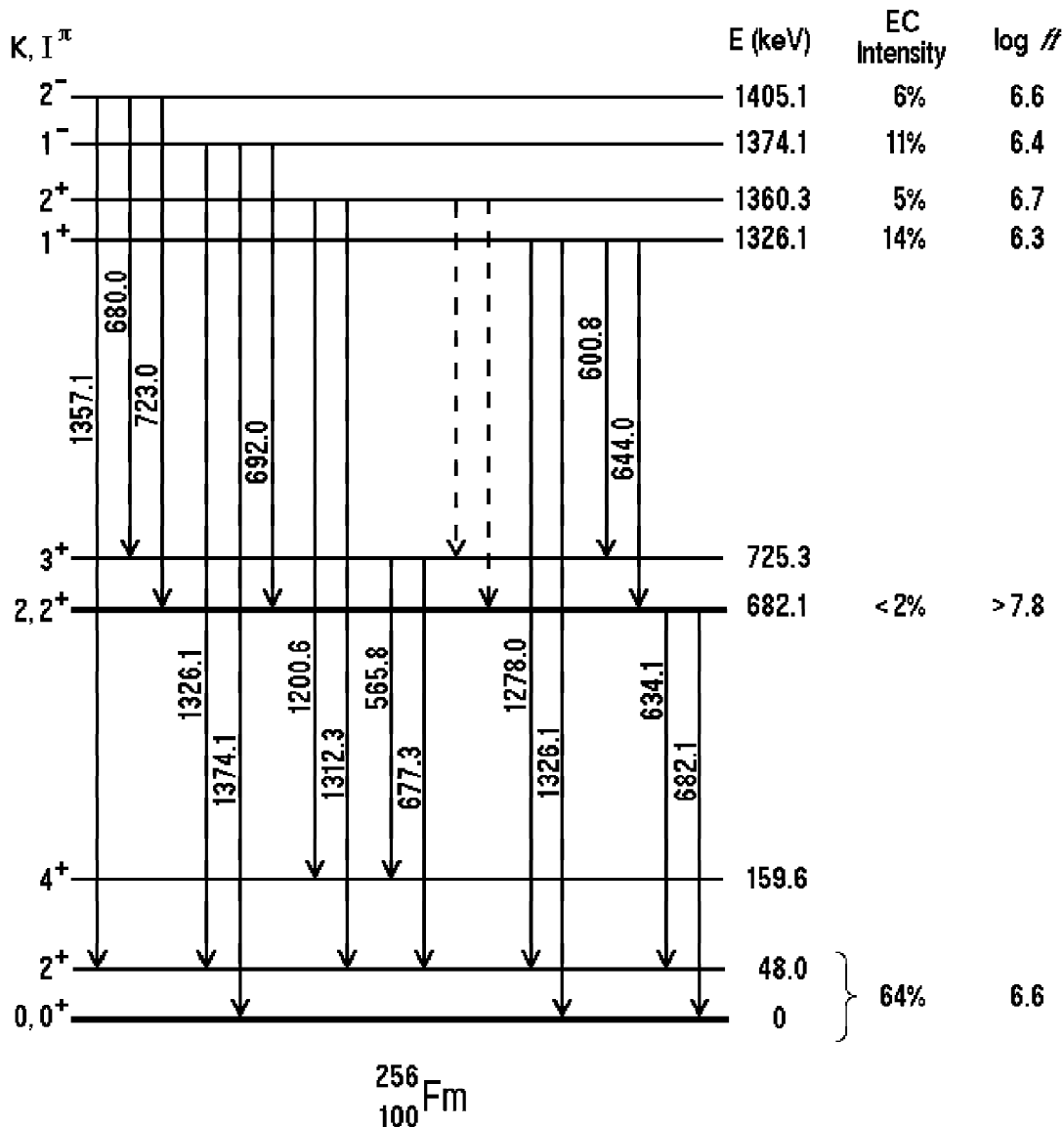


Fig. I-45. Electron capture decay scheme of  $^{256}\text{Md}$  deduced from the results of the present investigation. Dashed lines represent transitions expected but whose energies overlap with the stronger transitions.